COO-2271-33
CO - 2271 - 33

INTERACTION OF A DENSE FERMION MEDIUM WITH A SCALAR MESON FIELD

T. D. Lee and M. Margulies

Columbia University
New York, N. Y. 10027

This research was supported in part by the U. S. Atomic Energy Commission.

DISCLAIMER

ABSTRACT

The interaction between a dense Fermion medium and a scalar meson field is studied. It is shown that in the quasi-classical approximation, independently of the details of the theory, at low Fermion density the lowest energy state is normal (i.e., effective Fermion mass $m_{eff} \cong$ free mass), but at high density the state is abnormal (i.e., $m_{eff} \cong 0$). The nature of the transition is analysed at zero and low temperatures. Our main concern is to examine the problem of quantum fluctuation. Both the one- and two-loop diagrams are calculated. By developing a variational formalism involving only two-line irreducible diagrams, we derive a suitable high-density expansion for the energy. The quasi-classical solution emerges as the lowest order term in this expansion. Therefore, when the expansion is valid, the overall description of the transition given by the quasi-classical solution remains correct with the inclusion of quantum corrections.

CONTENTS

I. Introduction

Recently, it has been suggested[1, 2] that if there exists a strongly interacting 0+ meson, or resonance, then when the nucleon density becomes sufficiently high over an extended volume, there is the possibility of abnormal nuclear states, hitherto unobserved. A basic feature of the abnormal nuclear state is that in such a state the nucleon mass becomes zero (or nearly zero). Under suitable conditions, the abnormal nuclear states may be stable, or metastable. Furthermore, depending on the particular meson theory, as the nucleon density increases, the transition from the normal nuclear state to the abnormal nuclear state can be a sudden one, exhibiting the standard characteristics of a phase transition. So far, because of computational difficulties, the theoretical discussion of the abnormal nuclear state is restricted to a quasi-classical treatment only, similar to that used in a Thomas-Fermi model for the atomic system. Questions naturally arise as to other effects not included in such a quasi-classical solution, especially those related to quantum fluctuations because of multi-loop diagrams. The main purpose of this paper is to give a systematic analysis of these loop diagrams[3].

In order to understand the essential features of the problem involved, we shall consider only a simple renormalizable field theory in which there are two fields: a Boson field ϕ of spin 0 and a Fermion field ψ of spin $\frac{1}{2}$. [For applications to the nuclear system, ψ represents the nucleon field and ϕ some strongly interacting 0+ meson, or resonance.] The Lagrangian density is

$$\mathcal{L} = -\tfrac{1}{2}\left(\frac{\partial \phi}{\partial x_\mu}\right)^2 - U(\phi) - \psi^\dagger \gamma_4 \left[\gamma_\mu \frac{\partial}{\partial x_\mu} + (m + g\phi)\right] \psi + \text{counter terms} \tag{1.1}$$

where ϕ is Hermitian,

$$U(\phi) = \tfrac{1}{2} a\phi^2 + (3!)^{-1} b\phi^3 + (4!)^{-1} c\phi^4 \quad , \tag{1.2}$$

the parameters a, b, c, m and g are the appropriately defined renormalized constants, and the counter terms are for renormalization purposes. Through the transformation $\phi \to \phi +$ constant, one may always assume for the vacuum state

$$< \text{vac} \mid \phi(x) \mid \text{vac} > \; = \; 0 \tag{1.3}$$

where the vacuum state is defined to be the lowest eigenstate of the system with Fermion number 0. The total Fermion number $N \equiv \int \psi^\dagger \psi \, d^3r$ is, of course, conserved. Note that $U(\phi)$ does not contain a linear term in ϕ; consequently, there is a linear term in the counter terms. We assume the constant c to be positive so that $U(\phi)$ has a lower bound, and the constants a and b to satisfy

$$b^2 \leqq 3ac$$

so that the absolute minimum of $U(\phi)$ is at $\phi = 0$. For convenience, we shall quantize the system in a box of a finite volume Ω with the periodic boundary condition, and then take the limit $\Omega \to \infty$ in the end.

Let $\mid n >$ be the <u>lowest energy eigenstate</u> of the total Hamiltonian H that satisfies the constraint

$$\Omega^{-1} \int d^3r \, < n \mid \psi^\dagger \psi \mid n > \; \equiv \; n \tag{1.4}$$

where n denotes the average Fermion density. A useful concept is the energy density function $\mathcal{E}(n)$, related to the total Hamiltonian H by

$$\mathcal{E}(n) \equiv \lim_{\Omega\to\infty} \Omega^{-1} \langle n \mid H \mid n \rangle \ . \tag{1.5}$$

For practical applications to a finite but large nucleon system, $\mathcal{E}(n)$ denotes its volume energy. The simplest way to see why, for n sufficiently high, the system may exist in the abnormal state is to examine the quasi-classical solution.

Let us assume the Fermions to form a degenerate gas and ϕ to be described by a classical field. In such a quasi-classical treatment, we first examine the case that the Fermion density n is kept uniform in Ω. In the lowest energy state, the classical field ϕ must, then, be a constant. The corresponding energy density $\mathcal{E}(n)$ is given by

$$\mathcal{E} = U(\phi) + (4\pi^3)^{-1} \kappa \int_F d^3p \left[\vec{p}^2 + m_{eff}^2\right]^{\frac{1}{2}} \tag{1.6}$$

where m_{eff} is the effective mass of the Fermion, related to the free particle mass m by

$$m_{eff} = \left| m + g\phi \right| \ , \tag{1.7}$$

the subscript F next to the integral sign indicates that the integral extends only over the Fermi sea $|\vec{p}| \leq k_F$, and k_F is related to n by

$$k_F = (3\pi^2 n/\kappa)^{\frac{1}{3}} \tag{1.8}$$

with κ denoting the Fermion degeneracy due to its internal symmetry. For example,

$$\kappa = \begin{cases} 1 & \text{for a neutron medium} \\ 2 & \text{for a nuclear medium} \end{cases} \tag{1.9}$$

where, for simplicity, we assume equal numbers of protons and neutrons for the nuclear medium.

Throughout our discussion, we define the normal state to be one in which $m_{eff} \cong m$, and the abnormal state to be one in which $m_{eff} \cong 0$. As n increases, the Fermi-sea contribution to the energy becomes increasingly more important. Thus, for any given set of parameters a, b, c, g and m, in the high-density limit one finds by using (1.6),

$$\lim_{n\to\infty} \phi = -(m/g) \qquad \text{and} \qquad \lim_{n\to\infty} m_{eff} = 0 \ ; \tag{1.10}$$

i.e., the state becomes abnormal. On the other hand, in the low-density limit, because of (1.3), one must have

$$\lim_{n\to 0} \phi = 0 \qquad \text{and} \qquad \lim_{n\to 0} m_{eff} = m_N \ ;$$

i.e., the state is normal. As illustrated in Figure 1, depending on the parameters in the theory, the transition from the low-density "normal" solution ($m_{eff} \cong m$) to the high-density "abnormal" solution ($m_{eff} \cong 0$) may or may not be a continuous one. The details will be given in Section II. It will be shown there that one of the necessary conditions for a discontinuous transition is to have a sizable ϕ^3-coupling

$$b^2 > 2ac \ . \tag{1.11}$$

Of particular interest is the case of the σ-model[4], in which $b^2 = 3ac$. It has been shown in Refs. 1 and 2 that when the Fermion density n increases, the quasi-classical solution of the σ-model does produce a discontinuous transition from the normal state to the abnormal state. Further details concerning the nature of the phase transition will be given in Section II and in Appendix A.

Our main concern is to investigate the quantum correction to the quasi-classical solution. As will be shown, in a fully quantum mechanical treatment, the role of the constant classical field in the above quasi-classical solution is replaced by the average value

$$\bar{\phi} = \Omega^{-1} \int d^3r \, \langle n \mid \phi(x) \mid n \rangle \quad . \tag{1.12}$$

In the vacuum state $(n = 0)$, one has $\bar{\phi} = 0$; when $n \neq 0$, in the normal state, one has $\bar{\phi} \cong 0$, but in the abnormal state $\bar{\phi}$ is shifted to $\cong -(m/g)$. This shift in $\bar{\phi}$ is smallest in the strong-coupling limit, but largest in the weak-coupling limit. Thus, it seems reasonable that the quantum correction may also be smaller in the strong-coupling limit. Unfortunately, at present there exists no reliable technique that is capable of handling a relativistic quantum field theory with strong coupling (except in the totally fictitious two space-time dimensions, and even there only for a very few special examples[5]). As $g \to \infty$, it is not even clear whether the vacuum state does exist or not. The lack of knowledge concerning the vacuum state makes it difficult to discuss the quantum correction to the abnormal state in the strong coupling limit.

On the other hand, from the quasi-classical solution, the abnormal state is expected to exist even for a weakly-coupled meson field, provided the Fermion density is sufficiently high. Thus, it may be worthwhile to develop systematically the high-density but weak-coupling expansion of a Fermion medium interacting with a 0+ meson field. Some insight into the physical nature of the abnormal nuclear state and the related phase transition phenomenon may then be obtained. The actual task of establishing a systematic high-density, though weak-coupling, expansion turns out to be a non-trivial one. This is not surprising, since in the abnormal state the shift in $\bar{\phi}$ is $\cong -(m/g)$ which approaches

infinity as g becomes infinitesimal. The usual perturbation series is applicable only if the coupling is weak and the Fermion density remains relatively low. A suitable rearrangement of the usual perturbation series is therefore necessary in order to derive a high-density expansion.

We recall that in this problem both the energy density $\mathcal{E}(n)$ and the average field $\bar{\phi}$ depend on six parameters: a , b , c , m , g and the Fermi momentum k_F . Among these, only c and g^2 are dimensionless. Out of these six parameters, one may construct five dimensionless parameters:

$$g^2 \ , \quad \frac{g^2 k_F^2}{a} \ , \quad \frac{b^2}{ac} \ , \quad \frac{a}{m^2} \quad \text{and} \quad \frac{c}{g^2} \ . \qquad (1.13)$$

In the usual perturbation series, one expands in powers of g^2 , $(g k_F)^2$, b and c . [If k_F is $\ll m$, then $(g k_F)^2$ should be replaced by $(g k_F)^2 (k_F/m)$.] For the abnormal state, such a perturbation expansion is obviously inadequate. This is clear especially if we recall the condition on these parameters in the interesting case of a discontinuous transition. From (1.11), one sees that

$$\frac{b^2}{ac} \sim O(1) \ .$$

Furthermore, the Fermion density must be quite high, since on the one hand $\bar{\phi} \cong -(m/g)$ in the abnormal state, and on the other hand $\bar{\phi} \sim -(g k_F^2 m/a)$ from the field equation; it follows therefore

$$\frac{g^2 k_F^2}{a} \sim O(1) \ .$$

The appropriate high-density weak-coupling expansion that we are seeking is one in which, out of the five dimensionless parameters in (1. 13), only g^2 acts as the small expansion parameter. The other four parameters in (1. 13) are all regarded as $O(1)$; i.e.,

$$c \sim O(g^2) \ll 1 , \quad b^2 \sim O(ac)$$

and

$$a \sim O(m^2) \sim O(g^2 k_F^2) . \tag{1.14}$$

We may formally write in ascending powers of g^2:

$$\mathcal{E}(n) = \mathcal{E}_0 + \mathcal{E}_1 + \mathcal{E}_2 + \cdots \tag{1.15}$$

where

$$\mathcal{E}_0 \sim O(k_F^4) , \quad \mathcal{E}_1 \sim O(g^2 k_F^4) ,$$

$$\mathcal{E}_2 \sim O(g^4 k_F^4) \quad \text{or} \quad O(g^4 k_F^4 \ln g^2) , \quad \text{etc.} \tag{1.16}$$

To each order in g^2, or $g^2 \ln g^2$, the dependence of $\mathcal{E}(n)$ on the last four parameters in (1. 13) is supposed to be evaluated exactly. Because $k_F \sim O(m/g) \gg O(m)$, this weak coupling expansion is also a high-density expansion.

To derive such an expansion, we are helped by methods developed in many-body problems and statistical mechanics[6]. We will start, in Section III, from the usual perturbation series, and then sum over all one-line reducible graphs to obtain the well-known expansion in terms of the prototype diagrams[7]. The series of prototype diagrams is then further rearranged through a second summation over all two-line reducible graphs. The result is a variational formalism of $\mathcal{E}(n)$ in terms of the average field $\bar{\phi}$ and the two full

propagators: $D'(k)$ of the meson field and $S'(p)$ of the Fermion field. The details are given in Section IV. This variational formalism can then be used to give the desired high-density weak-coupling expansion.

As will be shown in Section IV C, if we neglect $O(g^4 k_F^4)$ and $O(g^4 k_F^4 \ln g^2)$ in the loop diagrams, the energy-density function becomes

$$\mathcal{E} = U(\bar{\phi}) + (4\pi^3)^{-1} \kappa \int_F d^3p \left[\vec{p}^2 + (m + g\bar{\phi})^2\right]^{\frac{1}{2}} + (64\pi^4)^{-1} \kappa g^2 k_F^4 \qquad (1.17)$$

where U is given by (1.2), and $\bar{\phi}$ is determined by the minimum of $\mathcal{E}$. We note that in the abnormal state $\bar{\phi} \sim -(m/g)$; therefore, $U(\bar{\phi}) \sim O(am^2/g^2)$, which is $\sim O(g^2 k_F^4)$ according to (1.14). In the above expression, the first two terms are exactly the same as the quasi-classical result provided that $\bar{\phi}$ replaces the classical field. The third term $(64\pi^4)^{-1} \kappa g^2 k_F^4$ is a new term, representing the quantum correction; more specifically, it is due to the change in the Fermion self-energy on account of the Fermi sea. [See (4.37) for the modification if there are, in addition to the 0+ meson, also pions.] Because it is independent of $\bar{\phi}$, (1.17) leads to the same dependence of $\bar{\phi}$ on the Fermion density as that in the quasi-classical solution. Thus, the overall description of the transition given by the quasi-classical solution remains correct in a quantum-mechanical treatment, at least when the expansion (1.15) is a valid one.

II. Quasi-classical Solution

In this section, we shall briefly review some of the properties of the quasi-classical solution.

A. General Discussion

In the quasi-classical solution, the Fermions are assumed to form a completely degenerate gas. We examine first the case that the Fermion density n is uniform inside the volume Ω. [The case of a non-uniform density will be discussed later in Section II B.] The meson field $\phi(x)$ is assumed to be classical. Since the Fermion density is kept everywhere the same, it is easy to see that in the lowest energy state the meson field must also be a constant. The energy density $\mathcal{E}(n)$ is given by (1.6), which may be written as

$$\mathcal{E}(n) = U_\phi + U_F \tag{2.1}$$

where

$$U_\phi \equiv U(\phi) = \tfrac{1}{2} a\phi^2 + (3!)^{-1} b\phi^3 + (4!)^{-1} c\phi^4 , \tag{2.2}$$

$$U_F = (4\pi^3)^{-1} \kappa \int_F d^3p \left[\vec{p}^2 + m_{eff}^2 \right]^{\frac{1}{2}} , \tag{2.3}$$

m_{eff} and κ are given respectively by (1.7) and (1.9).

As already stated in the introduction, from the above expression of $\mathcal{E}(n)$, it follows that, independent of the details of U_ϕ, at low density the system is normal (i.e., $\phi \cong 0$ and $m_{eff} \cong m$), while at sufficiently high density the system must become abnormal (i.e., $\phi \cong -m/g$ and $m_{eff} \cong 0$). The nature of the transition from the low-density "normal" solution to the high-density "abnormal" solution can be best analysed by examining the derivative of $\mathcal{E}(n)$. At any given n, the physical value of

ϕ is determined by minimizing $\mathcal{E}(n)$. Thus, it must be given by one of the solutions of

$$\frac{dU_\phi}{d\phi} = -\left(\frac{\partial U_F}{\partial \phi}\right)_n \quad . \tag{2.4}$$

Depending on the parameters a, b, c, m, g and n, Eq. (2.4) may have one, or three, or five solutions. We note that the left-hand side, $dU_\phi/d\phi$, is a cubic function of ϕ, independent of n, while the right-hand side, $-(\partial U_F/\partial\phi)_n$, is both an odd function of $m + g\phi$ and a monotonically decreasing function of ϕ, varying between the limiting value gn at $\phi = -\infty$ and $-gn$ at $\phi = +\infty$. As $n \to 0$, the minimum of $\mathcal{E}(n)$ is given by the solution $\phi \to 0$, and as $n \to \infty$ it is given by the solution $\phi \to -(m/g)$. When n varies, the transition between these two solutions may or may not be discontinuous. The necessary and sufficient condition for a discontinuous transition is to have a density n at which there should be two or more solutions of (2.4) in the open interval between $\phi = 0$ and $\phi = -(m/g)$. The proof is quite straightforward, as will be illustrated by the following examples:

1. If $b^2 < 2ac$, the function U_ϕ has no point of inflexion. Thus $dU_\phi/d\phi$ is a monotonically increasing function of ϕ, varying from $-\infty$ at $\phi = -\infty$ to $+\infty$ at $\phi = +\infty$. Equation (2.4) has only one solution, which gives the minimum of $\mathcal{E}(n)$; therefore, the physical value of ϕ varies continuously from $\phi = 0$ at $n = 0$ to $\phi = -(m/g)$ at $n = \infty$.

2. If b is of the opposite sign from g, the function $dU_\phi/d\phi$ is a monotonically increasing function at least in the region $g\phi < 0$; it varies from $-\infty$ at $g\phi = -\infty$ to 0 at $\phi = 0$. Thus, in the interval between $\phi = 0$ and $\phi = -(m/g)$, there is again only one solution of (2.4). Just like in the previous case, as n increases, the physical value of ϕ varies continuously from 0 to $-(m/g)$. [Both cases 1 and 2 are represented by (ii) in

Figure 1.]

3. Next, we examine the more interesting case when $b^2 > 2ac$ and b is of the same sign as g. Without any loss of generality, we may choose g positive, and therefore b also positive. There are two points of inflexion of U_ϕ, called A and B, where

$$\phi_A = c^{-1}\left[-b + (b^2 - 2ac)^{\frac{1}{2}}\right]$$

and (2.5)

$$\phi_B = c^{-1}\left[-b - (b^2 - 2ac)^{\frac{1}{2}}\right] .$$

If b^2 is also $> \frac{8}{3}ac$, then the curve $dU_\phi/d\phi$ has three zeroes, at $\phi = 0$, ϕ_+ and ϕ_- where

$$\phi_\pm = 3(2c)^{-1}\left[-b \pm (b^2 - \frac{8}{3}ac)^{\frac{1}{2}}\right] . \qquad (2.6)$$

Because of (1.3), U_ϕ has its absolute minimum at $\phi = 0$, a local maximum at ϕ_+ and a local minimum at ϕ_-. As shall be shown, provided that (m/g) is sufficiently large, there is always a discontinuous jump in ϕ as n increases. For clarity, we discuss separately the following possibilities:

(i) If $b^2 > \frac{8}{3}ac$ and $\phi = -(m/g)$ lies to the left of $\phi = \phi_+$, then the transition from the low-density solution, $\phi \to 0$, to the high-density solution, $\phi \to -(m/g)$, must be a discontinuous one.

In this case, at sufficiently low density, Eq. (2.4) has three solutions, labeled α, β and γ, which may be arranged in a descending order according to their ϕ-values; i.e.,

$$0 > \phi_\alpha > \phi_\beta > \phi_\gamma . \qquad (2.7)$$

In the interval between the origin and $\phi = -(m/g)$, depending on the position of $\phi = \phi_-$, one may have all these three solutions, or only two, α and β, as shown in case (i) of Figure 2. In either case, as $n \to 0$, the solution α approaches the origin; therefore, the minimum of $\mathcal{E}(n)$ is given by α. But as n increases, α approaches β. At a certain density, α and β coalesce, and above that density α disappears. Consequently, there must be a discontinuous transition.

(ii) If $b^2 > \frac{8}{3} ac$, but $\phi = -(m/g)$ lies to the right of the point of inflexion $\phi = \phi_A$, then as n increases, the physical value of ϕ varies continuously from 0 to $-(m/g)$.

In this case, between the origin and $\phi = -(m/g)$, Eq. (2.4) has only one solution, called α, as shown in case (ii) of Figure 2. It is not difficult to establish graphically that the shaded area $\alpha\beta A$ is always larger than the shaded area $\beta\gamma B$. Consequently, the minimum of $\mathcal{E}(n)$ is always given by α (never γ), and therefore, there is no discontinuity as n changes.

(iii) Similar considerations extend to the case when $b^2 > \frac{8}{3} ac$, but $\phi = -(m/g)$ lies in between ϕ_A and ϕ_+. As n varies, the transition from the solution $\phi = 0$ to $\phi = -(m/g)$ is a discontinuous one provided that at some density Eq. (2.4) has three solutions α, β and γ between the origin and $\phi = -(m/g)$, as shown in case (iii) of Figure 2. The discontinuity occurs when the two shaded areas $\alpha\beta A$ and $\beta\gamma C$ become equal. At low density, the absolute minimum of $\mathcal{E}(n)$ is given by α, but at high density by γ.

It can be shown that in this case a sufficient condition for a discontinuous transition is $(m/g) > \frac{1}{3}(b^2 - 2ac)^{-1}(b^3/c)$.

(iv) If $2ac < b^2 < \frac{8}{3} ac$, the transition from $\phi = 0$ to $\phi = -(m/g)$ may still be discontinuous, provided that $-(m/g)$ is sufficiently negative, as shown in case (iv) of Figure 2. The discontinuity occurs when the shaded areas $\alpha\beta A$ and $\beta\gamma B$ become equal.

B. σ - Model

Of particular interest is the σ-model[4]. For simplicity, we shall discuss the model only in the zero pion-mass limit. The σ-model consists of a spin $\frac{1}{2}$ nucleon field ψ, a spin 0 even parity field σ and the usual pseudoscalar field $\vec{\pi}$. The Lagrangian density is given by

$$\mathcal{L} = -\psi^\dagger \gamma_4 \gamma_\mu \frac{\partial \psi}{\partial x_\mu} - g\psi^\dagger \gamma_4 \left[\sigma + i\vec{\pi}\cdot\vec{\tau}\,\gamma_5\right]\psi$$

$$-\tfrac{1}{2}\left[\left(\frac{\partial\sigma}{\partial x_\mu}\right)^2 + \left(\frac{\partial\vec{\pi}}{\partial x_\mu}\right)^2\right] - \tfrac{1}{4}\lambda^2\left[\sigma^2 + \vec{\pi}^2 - \sigma_0^2\right]^2$$

$$+ \text{counter terms}. \qquad (2.8)$$

In the tree approximation, the free nucleon mass m_N and the free σ-meson mass m_σ are related to the parameters σ_0 and λ by

$$m_N = g\sigma_0 \quad \text{and} \quad m_\sigma = \sqrt{2}\,\lambda\sigma_0 \,. \qquad (2.9)$$

In the quasi-classical treatment, we may regard σ and $\vec{\pi}$ both as classical fields. As before, we first examine the case of a uniform nucleon density n. In the lowest energy state, both σ and $\vec{\pi}$ are then also uniform. The energy-density function is given by

$$\mathcal{E}(n) = U_\sigma + U_N \qquad (2.10)$$

where

$$U_\sigma = \tfrac{1}{4}\lambda^2(\sigma^2 + \vec{\pi}^2 - \sigma_0^2)^2 \,, \qquad (2.11)$$

$$U_N = (4\pi^3)^{-1}\kappa \int_F d^3p \left[\vec{p}^2 + m_{eff}^2\right]^{\frac{1}{2}} \,, \qquad (2.12)$$

$$m_{eff}^2 = g^2 (\sigma^2 + \vec{\pi}^2) \qquad (2.13)$$

and κ is given by (1.9). Equations (2.10)-(2.12) reduce respectively to the previous expression (2.1)-(2.3), if we set

$$\phi = (\sigma^2 + \vec{\pi}^2)^{\frac{1}{2}} - \sigma_0 \ , \qquad b^2 = 3ac \ ,$$

$$c = 6\lambda^2 \quad \text{and} \quad a = 2\lambda^2 \sigma_0^2 = m_\sigma^2 \ . \qquad (2.14)$$

[See (3.30) for the definition of a when radiative corrections are included.] By following the same argument given in the previous section, one finds that as the nucleon density n increases from zero, there is a discontinuous transition[1,2] from the normal state ($m_{eff} \cong m_N$) to the abnormal state ($m_{eff} \cong 0$), as illustrated by case (i) in Figure 1. Let n_c be the critical density. From (2.10)-(2.12), and by using a simple scale transformation, one sees that n_c in units of m_N^3 depends only on a single combination of parameters:

$$m_N^3 \, n_c^{-1} = f(\kappa g^2 m_N^2 / m_\sigma^2) \ . \qquad (2.15)$$

It is not difficult to calculate the explicit form of f. In Figure 3, we map out the region in $g^2/4\pi$ and m_σ for $n_c \leqq 2n_0$ where n_0 is the nuclear density in existing nuclei, given by

$$n_0^{-1} = \frac{4\pi}{3} (1.2 \text{ fm})^3 \ . \qquad (2.16)$$

For simplicity, we set the degeneracy factor $\kappa = 2$ for the nuclear matter. Although at present there is no reliable data on either m_σ or g^2, the range given in Figure 3 is not incompatible with most of the available discussions of 0+ resonances in the literature[4,8].

Since it is perhaps possible that through heavy ion collisions the nucleon density may increase from n_0 to about $2n_0$, this suggests that experimental investigations of abnormal nuclear states may become feasible.

Next, we investigate the lowest energy state of the system by allowing the nucleon density n to be non-uniform, of course keeping the total baryon number fixed. As the volume of the system $\Omega \to \infty$, the only way a non-uniform density may perhaps further lower the energy is to develop a two-phase region. This problem is closely connected to the question of the binding energy of the abnormal state. By setting $\sigma = 0$, one finds that for a uniform density, the total energy of the abnormal state is

$$E \equiv \Omega \mathcal{E} = \tfrac{3}{4} N k_F + \tfrac{1}{8} \Omega m_N^2 (m_\sigma^2/g^2) \qquad (2.17)$$

where $N = \Omega n$. At $(\partial E/\partial \Omega)_N = 0$, one obtains for the minimum of E

$$\frac{E}{N}_{min} = k_F = (\tfrac{3}{4})^{\frac{1}{3}} (m_N m_\sigma \pi/g) \qquad (2.18)$$

The binding energy per nucleon in the abnormal state is $m_N - k_F$. Thus, the system binds if

$$\frac{g^2}{4\pi} > \frac{3\pi}{16} \left(\frac{m_\sigma}{m_N}\right)^2 \qquad (2.19)$$

So far we have not considered the usual short-range nuclear forces. To make a thorough investigation of this important problem is quite beyond the scope of our present paper. Furthermore, one can show that in this case $\sigma = 0$ always corresponds to the absolute minimum of E. Let n_{Ab} be the corresponding density of the abnormal state at zero pressure. Because of (2.18), n_{Ab} is given by

$$n_{Ab} = \tfrac{1}{3}(2k_F^3/\pi^2) = (2\pi\sqrt{3})^{-\frac{1}{2}} (m_N m_\sigma/g)^{\frac{3}{2}} . \qquad (2.20)$$

Assuming that (2.19) is satisfied, for an average nucleon density $\Omega^{-1}N < n_{Ab}$, and Ω sufficiently large, one finds (now allowing the density to be non-uniform) the lowest energy state to consist of a two-phase region: a part of the volume, $\Omega - (N/n_{Ab})$, is empty and the rest in the abnormal state. The corresponding thermodynamic $p - v$ diagram is plotted in Figure 4 [diagram (i)], where p is the pressure and v is the specific volume,

$$v = N^{-1}\Omega \quad . \tag{2.21}$$

In this case, at zero temperature there is a first order phase transition at zero pressure. For $(4\pi)^{-1} g^2 < (3\pi/16)(m_\sigma/m_N)^2$, the abnormal state does not bind; even then, there is still a phase transition which, at zero temperature, occurs only under a finite pressure. Both possibilities are illustrated by diagrams (i) and (ii) in Figure 4.

Similar considerations can be readily extended to other zero-spin meson fields, different from the σ-model. It is important to note that high temperature[9] tends to destroy coherence. Throughout our discussions, we will concentrate only on zero, or low, temperature phenomena. A brief description of the thermodynamics functions at low but non-zero temperature is given in Appendix A. [See (A.15)-(A.18) for the expression of the two-phase region in the σ-model.]

So far we have not considered any of the usual short-range nuclear forces. To make a thorough investigation of this important problem is quite beyond the scope of our present paper. In Appendix B, a simplified "hard sphere" model is given, which we hope may illustrate in a qualitative way some of the problems involved.

III. Loop Diagrams

The Lagrangian density (1. 1) may be written as

$$\mathcal{L} = \mathcal{L}_0 + \mathcal{L}_1 + \text{counter terms} \tag{3.1}$$

where

$$\mathcal{L}_0 = -\tfrac{1}{2}\left(\frac{\partial\phi}{\partial x_\mu}\right)^2 - \tfrac{1}{2}a\phi^2 - \psi^\dagger \gamma_4 \left(\gamma_\mu \frac{\partial}{\partial x_\mu} + m\right)\psi \quad , \tag{3.2}$$

$$\mathcal{L}_1 = -(3!)^{-1} b\phi^3 - (4!)^{-1} c\phi^4 - g\phi\,\psi^\dagger \gamma_4 \psi \tag{3.3}$$

and

$$\begin{aligned}\text{counter terms} = {} & -(\delta J)\phi - \tfrac{1}{2}(\delta a)\phi^2 - (3!)^{-1}(\delta b)\phi^3 - (4!)^{-1}(\delta c)\phi^4 \\ & - (\delta m)\,\psi^\dagger\gamma_4\psi - (\delta g)\,\phi\,\psi^\dagger\gamma_4\psi - \tfrac{1}{2}(\delta Z_\phi)\left(\frac{\partial\phi}{\partial x_\mu}\right)^2 \\ & - (\delta Z_\psi)\,\psi^\dagger\gamma_4\gamma_\mu\frac{\partial\psi}{\partial x_\mu} \quad .\end{aligned} \tag{3.4}$$

The fields ϕ and ψ are the renormalized fields and the parameters a, b, c, g and m are the appropriately defined renormalized constants. In (3.4), δJ is determined by (1.3); the determinations of other counter terms depend on the precise definitions of the renormalized constants, which will be discussed later.

A. Perturbation Series

To analyse the systematics of the loop diagrams, we shall begin with the usual perturbation series by regarding ($\mathcal{L}_1$ + counter terms) as the perturbation. The zeroth order meson propagator $D(q)$ is, as usual,

$$D(q) = -i(q^2 + a - i\epsilon)^{-1} \tag{3.5}$$

where $q^2 = \vec{q}^2 - q_0^2$ and $\epsilon = 0+$. However, for a state with a nonzero Fermion density, the zeroth-order nucleon propagator $S(p)$ is given by[10]

$$S(p) = i\left[-i\gamma_\mu p_\mu - m + i\epsilon_n(p)\right]^{-1} \tag{3.6}$$

where $\epsilon_n(p)$ is a non-covariant function of the 4-momentum $p_\mu = (\vec{p}, ip_0)$ and the Fermi momentum k_F;

$$\epsilon_n(p) = 0- \quad \text{if } |\vec{p}| \leqq k_F \text{ and } p_0 > 0$$

and

$$\epsilon_n(p) = 0+ \quad \text{otherwise}. \tag{3.7}$$

In the zeroth-order solution of the groundstate $|n>$ for a Fermion density $n \neq 0$, all Fermion levels with energy $\omega_p \equiv (\vec{p}^2 + m^2)^{\frac{1}{2}} > 0$ and $|\vec{p}| \leqq k_F$ are occupied. Thus, in the complex p_0-plane, for $|\vec{p}| > k_F$ the poles of $S(p)$ are located as usual at $p_0 = \pm(\omega_p - i\epsilon)$, but for $|\vec{p}| \leqq k_F$ they are displaced to $p_0 = (\pm\omega_p) + i\epsilon$.

At zero Fermion density $n = 0$, the groundstate is $|\text{vac}>$ and therefore, because of (1.3), $\bar{\phi} = 0$ where $\bar{\phi}$ is defined by (1.12). If $n \neq 0$, then $\bar{\phi}$ is $\neq 0$. In Figure 5, we give the usual perturbation series expansion for $\bar{\phi}$ and $\mathcal{E}(n)$. In these diagrams, a solid line gives a factor $S(p)$, a dashed line a factor $D(k)$, and the various vertices give factors according to the explicit expressions of $\mathcal{L}_1$ and the counter terms. From (3.3), one sees that there is a ϕ^3 vertex carrying a factor $-ib$, a ϕ^4 vertex carrying a factor $-ic$, and another three-point $\phi\,\psi^\dagger\gamma_4\,\psi$ vertex carrying a factor $-ig$. In addition, there are vertices due to the counter terms given by (3.4). It is convenient to display explicitly the Fermion-number conservation by assigning each solid (Fermion) line an arrow, indicating the flow of the Fermion number, but none to the dashed (meson)

line. In addition, each diagram carries a factor s^{-1} where s is its symmetry number, and each Fermion loop gives a factor (-1).

To derive the symmetry number, let us consider a diagram with ℓ_F internal Fermion lines and ℓ_M internal meson lines. The total number of internal lines is

$$\ell = \ell_F + \ell_M \quad . \tag{3.8}$$

We first assign to each end of every internal line a different integer 1, or 2, $\cdots$, or 2ℓ. The resulting diagram is called a "numbered diagram". We then consider the $(2\ell)!$ permutations of these 2ℓ integers. The total number of permutations that leave the "numbered diagram" unchanged is the symmetry number. [Because the Fermion lines carry arrows but the meson lines do not, there is an alternative way to derive the symmetry number. We may assign only one number to every Fermion line, but as before, two numbers to every meson line, one for each end. There are altogether $\ell_F + 2\ell_M$ numbers assigned. Next we consider the product of the $\ell_F!$ permutations between the numbers associated with the Fermion lines times the $(2\ell_M)!$ permutations between the numbers associated with the ends of the meson lines. Among the $\ell_F! \times (2\ell_M)!$ permutations, the total number of permutations that leave the "numbered diagram" invariant is the same symmetry number s defined before.] See Figure 6 for the symmetry number of some sample diagrams.

It is useful to introduce the concept of "L-line reducibility". [Actually, we are only interested in the special cases of $L = 1$ and 2.] We call a diagram "L-line reducible" if it can be separated into two or more disconnected parts by cutting L different internal lines open; otherwise, it is called "L-line irreducible". From this definition, it follows that if a diagram is two-line irreducible, then it is also one-line irreducible; the

converse is, of course, not true. For example, in Figure 5, the first two rows of diagrams for $\mathcal{E}(n)$ are all one-line reducible, therefore also two-line reducible; on the third row, only the first one is two-line irreducible (and therefore also one-line irreducible); on the fourth row, the first one is two-line reducible, though one-line irreducible.

The partial sum over all one-line reducible diagrams can be readily carried out[6], which leads to the familiar expression in terms of the prototype diagrams[7]. Each prototype diagram is one-line irreducible, and vice versa.

B. Prototype Diagrams

A simple way to derive the series expansion of $\mathcal{E}(n)$ in terms of the prototype diagrams is to introduce

$$\chi \equiv \phi - \bar{\phi} \ , \tag{3.9}$$

so that in the groundstate $|\, n >$

$$\bar{\chi} \equiv \Omega^{-1} \int d^3r \, < n \,|\, \chi(x) \,|\, n > \; = \; 0 \quad . \tag{3.10}$$

The Lagrangian density (3.1) can then be written as

$$\begin{aligned} \mathcal{L} \; = \; & -\tfrac{1}{2}\left(\frac{\partial \chi}{\partial x_\mu}\right)^2 - \; U(\bar{\phi}) \; - \tfrac{1}{2}\, \bar{a}\, \chi^2 - \; (3!)^{-1}\, \bar{b}\, \chi^3 - \; (4!)^{-1}\, \bar{c}\, \chi^4 \\ & - \psi^\dagger \gamma_4 \left(\gamma_\mu \frac{\partial}{\partial x_\mu} + \bar{m} + g\chi \right) \psi \; + \; \text{counter terms} \end{aligned} \tag{3.11}$$

where

$$\bar{a} \; = \; d^2U/d\bar{\phi}^2 \; = \; a + b\bar{\phi} + \tfrac{1}{2}\, c\bar{\phi}^2 \quad ,$$

$$\bar{b} = d^3U/d\bar{\phi}^3 = b + c\bar{\phi} \quad ,$$

$$\bar{c} = c \qquad \text{and} \qquad \bar{m} = m + g\bar{\phi} \quad . \tag{3.12}$$

The counter terms are now given by

$$\begin{aligned} \text{counter terms} = & -\delta U(\bar{\phi}) - (\delta\bar{J})X - \tfrac{1}{2}(\delta\bar{a})X^2 - (3!)^{-1}(\delta\bar{b})X^3 \\ & -(4!)^{-1}\delta\bar{c}\,X^4 - (\delta\bar{m})\,\psi^\dagger\gamma_4\psi - (\delta g)\,X\,\psi^\dagger\gamma_4\psi \\ & -\tfrac{1}{2}\delta Z_\phi\left(\frac{\partial X}{\partial x_\mu}\right)^2 - (\delta Z_\psi)\,\psi^\dagger\gamma_4\gamma_\mu\frac{\partial\psi}{\partial x_\mu} \end{aligned} \tag{3.13}$$

where

$$\delta U = (\delta J)\bar{\phi} + \tfrac{1}{2}(\delta a)\bar{\phi}^2 + (3!)^{-1}(\delta b)\bar{\phi}^3 + (4!)^{-1}(\delta c)\bar{\phi}^4 \quad ,$$

$$\delta\bar{J} = d(U+\delta U)/d\bar{\phi} \quad , \qquad \delta\bar{a} = d^2(\delta U)/d\bar{\phi}^2 \quad ,$$

$$\delta\bar{b} = d^3(\delta U)/d\bar{\phi}^3 \quad , \qquad \delta\bar{c} = \delta c \quad ,$$

and

$$\delta\bar{m} = \delta m + (\delta g)\bar{\phi} \quad . \tag{3.14}$$

Since the above Lagrangian density depends explicitly on $\bar{\phi}$, so would the energy levels. The physical value of $\bar{\phi}$ is determined by the condition (3.10).

By using (3.11), one can readily expand $\mathcal{L}(n)$ in a new perturbation series by regarding $\bar{b}$, $\bar{c}$ and g as the perturbations. The zeroth order meson propagator and Fermion propagator are now respectively given by, instead of (3.5) and (3.6),

$$\bar{D}(q) = -i\left[q^2 + \bar{a} - i\epsilon\right]^{-1} \tag{3.15}$$

and

$$S(p) = i\left[-i\gamma_\mu p_\mu - \bar{m} + i\epsilon_n(p)\right]^{-1} \tag{3.16}$$

where $\epsilon = 0+$ and $\epsilon_n(p)$ is given by (3.7).

To derive the zeroth order energy, we adopt the usual convention that the vacuum energy is zero. Since the vacuum state is defined to be the groundstate in the case of zero Fermion density (i.e., $n = 0$), we have

$$\mathcal{E}(0) = 0 \ . \tag{3.17}$$

By using (3.11), one finds that to zeroth order in b, $\bar{c}$ and g the groundstate energy density $\mathcal{E}(n)$ for $n \neq 0$ is given by

$$\mathcal{E}_{q.cl.} + \Delta\mathcal{E}_{vac} \tag{3.18}$$

where $\mathcal{E}_{q.cl.}$ is the previously obtained quasi-classical expression

$$\mathcal{E}_{q.cl.} = U(\bar{\phi}) + (8\pi^3)^{-1} \int_F (2\kappa)\, d^3p\, (\vec{p}^2 + \bar{m}^2)^{\frac{1}{2}} \ , \tag{3.19}$$

and $\Delta\mathcal{E}_{vac}$ is the change in the vacuum energy due to $\bar{\phi} \neq 0$,

$$\begin{aligned}\Delta\mathcal{E}_{vac} = &- (8\pi^3)^{-1} \int (2\kappa)\, d^3k \left[(\vec{k}^2 + \bar{m}^2)^{\frac{1}{2}} - (\vec{k}^2 + m^2)^{\frac{1}{2}}\right] \\ &+ (8\pi^3)^{-1} \int \tfrac{1}{2} d^3k \left[(\vec{k}^2 + \bar{a})^{\frac{1}{2}} - (\vec{k}^2 + a)^{\frac{1}{2}}\right] \\ &+ \text{subtraction}\end{aligned} \tag{3.20}$$

in which the first term is the energy change of the "Fermion negative sea" and the second term is the change in the "zero-point meson energy"; both are divergent, but finite results

can emerge if we subtract out an appropriate fourth order polynomial in $\bar{\phi}$ due to renormalization. [See (3.22) below.]

The higher order corrections can be derived in terms of diagrams by using (3.11), (3.15) and (3.16). We may write for the energy density

$$\mathcal{E}(n, \bar{\phi}) = \mathcal{E}_{q.cl.} + \Delta\mathcal{E}_{vac} + \sum_{\ell=2}^{\infty} \mathcal{E}_{\ell\text{-loop}} \tag{3.21}$$

in which $\mathcal{E}$ depends explicitly on $\bar{\phi}$. Because $\bar{X} = 0$, it can be readily seen that all loop diagrams are <u>one-line irreducible.</u> In Figure 6 examples of two-loop and three-loop diagrams, together with their symmetry numbers, are listed. The counter terms $\delta\bar{m}$, δZ_ψ, $\delta\bar{a}$, $\cdots$ can always be re-expressed as sums of loop diagrams in terms of the renormalized constants $\bar{a}$, $\bar{b}$, $\bar{c}$, $\bar{m}$, $\bar{g}$ and $\bar{\phi}$. In (3.21), for diagrams involving counter terms, we find it convenient to define "ℓ-loop" to include also these loops in the counter terms. Because of this definition, there is no one-loop diagram in the sum over $\mathcal{E}_{\ell\text{-loop}}$. [An otherwise "one-loop" diagram with counter terms $\delta\bar{m}$, $\delta\bar{a}$, $\cdots$ as vertices is here considered as a two-, or more, loop diagram.]

It may be instructive to compare the above series (3.21), which is in terms of one-line irreducible diagrams (i.e., prototype diagrams), with the original perturbation series expansion discussed in the previous section. By using Figure 5, one can express $\mathcal{E}(n)$ in terms of $\bar{\phi}$; one finds then, as usual, $U(\bar{\phi})$ comes from the sum of the tree diagrams, while $\Delta\mathcal{E}_{vac}$ comes from the sum of all one-loop diagrams. In (3.21), however, both terms come from the zeroth order energy calculation of the Lagrangian (3.11). The explicit form of the vacuum-energy change is[1,7]

$$\Delta\mathcal{E}_{vac} = -(16\pi^2)^{-1}\,\kappa\,\bar{m}^4 \ln(\bar{m}^2/m^2) + (64\pi^2)^{-1}\,\bar{a}^2 \ln(\bar{a}/a) + \text{a finite fourth order polynomial in } \bar{\phi} \tag{3.22}$$

where $\bar{m} = m + g\bar{\phi}$ and $\bar{a} = a + b\bar{\phi} + \frac{1}{2} c\bar{\phi}^2$. There is a certain arbitrariness in the choice of the fourth order polynomial, depending on the precise definitions of the renormalized constants a, b and c. Different polynomials correspond simply to different choices of a, b and c. Among all possible conventions, the following is a particularly simple one:

Let us first consider the σ-model. Its Lagrangian (2.8) is invariant under a discrete 0_4 rotation:

$$\sigma \to -\sigma \quad , \quad \vec{\pi} \to -\vec{\pi}$$

and

$$\psi \to \gamma_5 \psi \quad . \tag{3.23}$$

A similar invariance exists even if there is no pion, provided that the constants a, b and c for the 0+ field $\phi \equiv \sigma - \sigma_0$ satisfy (2.14) where $\sigma_0 = (m/g)$. The corresponding symmetry becomes, instead of (3.23), simply a reflection:

$$\sigma \to -\sigma \qquad \text{and} \qquad \psi \to \gamma_5 \psi \quad . \tag{3.24}$$

In either case, $\Delta\mathcal{E}_{vac}$ should be, like

$$U(\bar{\sigma}) = \frac{\lambda^2}{4} (\bar{\sigma}^2 - \sigma_0^2)^2 \quad , \tag{3.25}$$

an even function of $\bar{\sigma}$, which is the expectation value of the σ-field. Since $\bar{m} = g\sigma$,

$$\bar{a} = \lambda^2 (3\bar{\sigma}^2 - \sigma_0^2) \tag{3.26}$$

and $\bar{\phi} = \bar{\sigma} - \sigma_0$, one sees that in order to have $\Delta\mathcal{E}_{vac}$ as an even function of $\bar{\sigma}$, the fourth order polynomial in (3.22) must be even in $\bar{\sigma}$. On account of (3.26), this is mathematically equivalent to writing (3.22) in the form

$$\Delta \mathcal{E}_{vac} = -(16\pi^2)^{-1} \kappa \bar{m}^4 \ln(\bar{m}^2/m^2) + (64\pi^2)^{-1} \bar{a}^2 \ln(\bar{a}/a) + \text{a quadratic function in } \bar{a} \ , \qquad (3.27)$$

in which the quadratic function can be determined by requiring

$$\text{at } \bar{\phi} = 0 \ , \quad \Delta \mathcal{E}_{vac} = 0 \ ,$$

$$\frac{d}{d\bar{\phi}} (\Delta \mathcal{E}_{vac}) = 0 \quad \text{and} \quad \frac{d^2}{d\bar{\phi}^2} (\Delta \mathcal{E}_{vac}) = 0 \ . \qquad (3.28)$$

Thus, when the Fermion density $n = 0$, $\bar{\phi} = 0$ is a minimum of $\mathcal{E}$. [In the σ-model, $\bar{\phi} = 0$ corresponds to $\bar{\sigma} = \sigma_0$.] Just as in Ref. 1, we shall require (3.27) and (3.28) to hold in <u>general</u> [11], not just in the σ-model. The result for an arbitrary $U(\phi)$ is

$$\Delta \mathcal{E}_{vac} = -(16\pi^2)^{-1} \kappa \bar{m}^4 \ln(\bar{m}^2/m^2) + (64\pi^2)^{-1} \bar{a}^2 \ln(\bar{a}/a) + \tfrac{1}{2} \alpha (\bar{a} - a)^2 + \beta (\bar{a} - a) \qquad (3.29)$$

where

$$\alpha = (8\pi^2 b)^{-1} \left[\kappa g (m/b)^2 (7gb - mc) - \frac{3}{8} b \right]$$

and

$$\beta = (8\pi^2 b)^{-1} \left(\kappa g m^3 - \frac{1}{8} ab \right) \ .$$

Throughout our discussion, the renormalization is carried out at $k_\mu = 0$. Thus, the renormalized constants m and a are defined by

$$m = -i \lim_{k_\mu = 0} \lim_{n=0} \left[S'(k) \right]^{-1}$$

and

$$a = -i \lim_{k_\mu = 0} \lim_{n=0} \left[D'(k) \right]^{-1} \qquad (3.30)$$

where $S'(k)$ and $D'(k)$ denote respectively the <u>full</u> renormalized Fermion- and meson-

propagators. Because of radiative corrections m and $a^{\frac{1}{2}}$ are <u>not</u> the same as the physical free Fermion- and free meson-masses.

For the σ-model, (3.29) becomes

$$\begin{aligned}\Delta\mathcal{E}_{vac} = &- (8\pi^2)^{-1} (g\bar{\sigma})^4 \ln(\bar{\sigma}^2/\sigma_0^2) + (64\pi^2)^{-1} \bar{a}^2 \ln(\bar{a}/a) \\ &+ (16\pi^2)^{-1} 3g^4 \left[1 - \frac{9}{32}(a^2/m^4)\right](\bar{\sigma}^2 - \sigma_0^2)^2 \\ &+ (8\pi^2)^{-1} g^2 m^2 \left[1 - \frac{3}{16}(a^2/m^4)\right](\bar{\sigma}^2 - \sigma_0^2) \qquad (3.31)\end{aligned}$$

where $\bar{a}$ is given by (3.26) and, for simplicity, we set the degeneracy factor $\kappa = 2$. It is of interest to observe that for $a \approx 1.4\, m^2$, even for a relatively large $(4\pi)^{-1} g^2$, $\Delta\mathcal{E}_{vac}$ remains relatively small over a fairly wide range of $\bar{\sigma}$. [See Figure 7.]

For $\bar{\sigma}^2 < \frac{1}{3}\sigma_0^2$, $\bar{a}$ becomes < 0 and therefore $\Delta\mathcal{E}_{vac}$ is complex. As will be shown in the next section, one should have used the full meson propagator $D'(k)$ instead of $\bar{D}(k)$, and this would lead to replacing $\bar{a} = -i\left[\bar{D}(0)\right]^{-1}$ by the positive definite

$$a' \equiv -i\left[D'(0)\right]^{-1} . \qquad (3.32)$$

That

$$a' > 0 \qquad (3.33)$$

can be established by using

$$D'(k) = \int d^4x \exp(i k_\mu x_\mu) \langle n \mid T\, X(x)\, X(0) \mid n \rangle , \qquad (3.34)$$

in the Heisenberg representation, where $X = \sigma - \bar{\sigma}$ in the σ-model (or $\phi - \bar{\phi}$ in the general case) and T denotes the time-ordered product; (3.33) then follows from the usual positivity requirement of the spectral representation of $D'(k)$. At zero nucleon

density, $a' = a$ according to (3.30). To have a rough idea of the variation of vacuum energy-change versus $\bar{\sigma}$ for $\bar{\sigma}^2 < \frac{1}{3}\sigma_0^2$, we may simply replace $\bar{a}$ by a' in (3.31), but (rather arbitrarily) without including any other changes; $\Delta\mathcal{E}_{vac}$ becomes then

$$\begin{aligned}\Delta\mathcal{E}'_{vac} \equiv & -(8\pi^2)^{-1}(g\bar{\sigma})^4 \ln(\bar{\sigma}^2/\sigma_0^2) + (64\pi^2)^{-1} a'^2 \ln(a'/a) \\ & + (16\pi^2)^{-1} 3g^4 \left[1 - \frac{9}{32}(a^2/m^4)\right](\bar{\sigma}^2 - \sigma_0^2)^2 \\ & + (8\pi^2)^{-1} g^2 m^2 \left[1 - \frac{3}{16}(a^2/m^4)\right](\bar{\sigma}^2 - \sigma_0^2) \end{aligned} \tag{3.35}$$

where, as can be readily verified, if one neglects higher order radiative corrections,

$$a' = \bar{a} + (2\pi^3)^{-1} g^2 \int_F (\vec{p}^2 + g^2\bar{\sigma}^2)^{-\frac{3}{2}} \vec{p}^2 \, d^3p \ . \tag{3.36}$$

In Figure 7, besides $\Delta\mathcal{E}_{vac}$, we also plot $\Delta\mathcal{E}'_{vac}$ versus $\bar{\sigma}$ for $a = 1.4\ m^2$, $(4\pi)^{-1} g^2 = 5$ and $n = 6\, n_0$, where $n_0^{-1} = \frac{1}{3} 4\pi (1.2\ fm)^3$. These plots illustrate the cancellation between the vacuum energy-change of the mesons and that of the Fermions when a is near $1.4\ m^2$.

Returning now to the general problem of a 0+ meson ϕ with an arbitrary fourth order polynomial $U(\phi)$, we note that since the Lagrangian density (3.11) depends on $\bar{\phi}$, so does the energy density $\mathcal{E}(n, \bar{\phi})$. As mentioned before, the physical value of $\bar{\phi}$ is determined by the requirement $\bar{X} = 0$. The following theorem shows that this is equivalent to minimizing $\mathcal{E}(n, \bar{\phi})$ with respect to $\bar{\phi}$.

Theorem 1. At the physical value of $\bar{\phi}$, one has

$$\frac{\partial}{\partial\bar{\phi}} \mathcal{E}(n, \bar{\phi}) = 0 \tag{3.37}$$

and

$$\frac{\partial^2}{\partial \bar{\phi}^2} \mathcal{E}(n, \bar{\phi}) > 0 \qquad (3.38)$$

where $\mathcal{E}(n, \bar{\phi})$ is given by (3.21), and in the differentiation the original renormalized constants a, b, c, m and g together with the original counter terms δa, δb, δc, $\cdots$ are all kept fixed.

Proof. Under the variation $\bar{\phi} \to \bar{\phi} + d\bar{\phi}$, because of (3.12), (3.15) and (3.16),

$$\begin{aligned} \bar{D}(k) &\to \bar{D}(k) - i\bar{b}\left[\bar{D}(k)\right]^2 d\bar{\phi} , \\ \bar{S}(p) &\to \bar{S}(p) - ig\left[\bar{S}(p)\right]^2 d\bar{\phi} , \\ \bar{b} &\to \bar{b} + c(d\bar{\phi}) \end{aligned} \qquad (3.39)$$

and similar variations for the counter terms $\delta\bar{a}$, $\delta\bar{b}$, etc. By definition, the loop diagrams for $\mathcal{E}(n, \bar{\phi})$ are all without external lines. From (3.39), one sees that under the $\bar{\phi}$-variation, to first order in $d\bar{\phi}$, the loop diagrams all turn into diagrams with a single external meson line, which carries an amplitude $d\bar{\phi}$ and a zero 4-momentum. Upon comparison with the original power series expansion of $\bar{\phi}$, given in Figure 5, one can readily verify that (3.37) and $\bar{X} = 0$ are the same condition. Similarly, one finds that to $(d\bar{\phi})^2$, the same variation in $\bar{\phi}$ turns every loop diagram into a meson-propagator diagram at zero 4-momentum. Through a straightforward diagram-counting, one can show that

$$\frac{\partial^2}{\partial \bar{\phi}^2} \mathcal{E}(n, \bar{\phi}) = -i\left[D'(0)\right]^{-1} . \qquad (3.40)$$

The inequality (3.38) follows on account of (3.32) and (3.33). Theorem 1 is then proved.

The evaluation of the two-loop diagrams is straightforward, though tedious. From Figure 6, we see that, apart from diagrams involving counter terms, there are only three two-loop prototype diagrams. Among these, the second and the third do not explicitly depend on k_F. These two diagrams have already been calculated; they are given by Eq. (3.17) of Ref. 1. The evaluation of the first two-loop diagram in Figure 6 turns out to be rather complicated. We may separate the result into a sum of three terms, in descending order of their explicit dependence on k_F: $O(k_F^4) + O(k_F^2) + O(k_F^0)$. The complete expression is quite long. Here, we give only the term proportional to k_F^4. For a single 0+ field ϕ, with arbitrary constants a, b and c, we find the two-loop contribution to be

$$\left[\mathcal{E}_{2\text{-loop}}\right]_{\phi} = (64\pi^4)^{-1} \kappa g^2 k_F^4 + O(k_F^2) \quad . \tag{3.41}$$

For the σ-model, after including the effect of pion fields and setting $\kappa = 2$, we find

$$\left[\mathcal{E}_{2\text{-loop}}\right]_{\sigma} = -(16\pi^4)^{-1} g^2 k_F^4 + O(k_F^2) \quad . \tag{3.42}$$

The details are given in Appendix C. As will be seen there, (3.41) and (3.42) are due to the change in the Fermion self-energy because of the exclusion principle and the presence of the Fermi sea.

IV. Two-line Irreducible Diagrams

For theories with a sizable $b\phi^3$ coupling, e.g., the σ-model, in the abnormal state $\bar{\phi} \cong -(m/g)$ the sign of $\bar{a} = d^2 U(\bar{\phi})/d\bar{\phi}^2$ may become negative. [See case (i) of Figure 1.] The series in terms of prototype diagrams is then obviously inadequate, since its zeroth order meson propagator $\bar{D}(k)$ would have a tachyon pole! On the other hand, as discussed in the previous section, the full meson propagator $D'(k)$ always satisfies the positivity requirement: $a' = -i/D'(0)$ is always positive, even though $\bar{a} = -i/\bar{D}(0)$ may not be. Thus, it seems sensible to expand the energy density function $\mathcal{E}(n)$ in terms of the full meson propagator $D'(k)$.

A. Variational Principle

The technique of expansion in terms of the full propagator has been developed[6] for quite some time for problems in statistical mechanics and many-body systems. The same technique can be readily extended to the present problem[3]. We may start from the Lagrangian density (3.11), and expand $\mathcal{E}(n)$ formally first in terms of the prototype diagrams, as before. These diagrams are all without external lines. We then perform a partial sum over all two-line reducible diagrams. This leads to a formulation of $\mathcal{E}(n)$ as a sum over only <u>two-line irreducible diagrams</u>. In each diagram, the Feynman rule is modified: every meson (dashed) line now carries a factor $D'(k)$, the full renormalized meson propagator, and every Fermion (solid) line carries a factor $S'(p)$, the full renormalized Fermion propagator. By definition, there is no two-point vertex in a two-line irreducible diagram; there are only three- and four-point vertices in these diagrams. These vertices carry the same factors as the corresponding ones in the prototype diagrams; i.e., there are the $b\chi^3$,

$\bar{c}X^4$ and $g\psi^\dagger\gamma_4\psi X$ vertices, as well as other three- and four-point vertices due to the counter terms, given by (3.13). For simplicity, in the following we shall consider the sum $\bar{b}+\delta\bar{b}$ as one vertex, and similarly for $\bar{c}+\delta\bar{c}$ and $g+\delta g$.

Definition 1. We first define a functional f_ℓ of D' and S' by

$$-i f_\ell(D', S') \equiv \text{sum of all } \ell\text{-loop two-line irreducible diagrams}. \tag{4.1}$$

There are only three $\ell = 2$ two-line irreducible diagrams, all given in Figure 6, and four $\ell = 3$ two-line irreducible diagrams, which are given by the first four three-loop diagrams in Figure 6.

Definition 2. Next, we define another functional

$$\begin{aligned} F(D',S') \equiv\ & U(\bar{\phi}) + (8\pi^3)^{-1} \int_F (2\kappa)\, d^3p\, (\vec{p}^2 + m_0^2)^{\frac{1}{2}} \\ & - i(2\pi)^{-4} \int d^4p\ \text{trace}\left\{\ln\left[S'(p)/S_0(p)\right] - \left[S'(p)/\bar{S}_0(p)\right] + 1\right\} \\ & + \tfrac{1}{2} i(2\pi)^{-4} \int d^4k \left\{\ln\left[D'(k)/D_0(k)\right] - \left[D'(k)/\bar{D}_0(k)\right] + 1\right\} \\ & + \sum_{\ell=2}^{\infty} f_\ell(D', S') + \text{subtraction term} \end{aligned} \tag{4.2}$$

where $U(\bar{\phi})$ is given by (1.2), m_0 is the unrenormalized mass

$$m_0 = (1+\delta Z_\psi)^{-1}(m+\delta m)\ , \tag{4.3}$$

and S_0, D_0, $\cdots$ are various unrenormalized propagators defined by

$$S_0(p) = i\left[(1+\delta Z_\psi)(-i\gamma_\mu p_\mu) - m - \delta m + i\epsilon_n\right]^{-1}\ , \tag{4.4}$$

$$D_0(k) = -i\left[(1+\delta Z_\phi)k^2 + a + \delta a - i\epsilon\right]^{-1}\ , \tag{4.5}$$

$$\bar{S}_0(p) = i\left[(1+\delta Z_\psi)(-i\gamma_\mu p_\mu) - \bar{m} - \delta\bar{m} + i\epsilon_n\right]^{-1} , \tag{4.6}$$

and

$$\bar{D}_0(k) = -i\left[(1+\delta Z_\phi)k^2 + \bar{a} + \delta\bar{a} - i\epsilon\right]^{-1} . \tag{4.7}$$

In (4.2), the subtraction term is a fourth order polynomial in $\bar{\phi}$; it differs from δU [given by (3.14)] by an additive constant:

$$\text{subtraction term} = \delta U + \text{constant} , \tag{4.8}$$

where the constant is to be chosen such that when, later on, F is used for evaluating $\mathcal{E}(n)$, one has, at $n=0$, $\mathcal{E}(0)=0$.

Theorem 2. The correct full renormalized propagators $D'(k)$ and $S'(p)$ are determined by

$$\frac{\delta}{\delta D'(k)} F(D', S') = 0 \tag{4.9}$$

and

$$\frac{\delta}{\delta S'(p)} F(D', S') = 0 \tag{4.10}$$

in which $\bar{\phi}$ and n are kept fixed. Furthermore, when D' and S' assume their correct forms, the functional $F(D', S')$ is equal to the energy-density function $\mathcal{E}(n)$. [The matrix $S'(p)$ may be written as $A + (-i\gamma_\mu p_\mu)B$ where A and B are c. no. functions. In (4.10), it is understood that $\delta S' = \delta A + (-i\gamma_\mu p_\mu)\delta B$.]

Proof. The proof of this theorem follows closely that of a similar theorem[6] in statistical mechanics and many-body problems. From the definition of F, it follows that (4.9) and (4.10) imply

$$\left[D'(k)\right]^{-1} - \left[\bar{D}_0(k)\right]^{-1} = 2i(2\pi)^4 \frac{\delta}{\delta D'(k)} \sum_{\ell=2}^{\infty} f_\ell(D', S') \tag{4.11}$$

and

$$\left[S'(p)\right]^{-1} - \left[\bar{S}_0(p)\right]^{-1} = -i\,(2\pi)^4 \frac{\delta}{\delta S'(p)} \sum_{\ell=2}^{\infty} f_\ell(D', S') \quad . \tag{4.12}$$

Through iterations, the solutions D' and S' can be expressed in terms of $\bar{D}_0$ and $\bar{S}_0$, or $\bar{D}$ and $\bar{S}$ [introduced in (3.15) and (3.16)]. By comparing with the series expansion of D' and S' in terms of prototype diagrams, one can readily establish that the solutions of (4.11) and (4.12) are indeed the full renormalized propagators D' and S'.

It is useful to define

$$\begin{aligned} G(D', S') \equiv & -i\,(2\pi)^{-4} \int d^4p\ \text{trace}\left\{\ln\left[S'(p)/\bar{S}_0(p)\right] - \left[S'(p)/\bar{S}_0(p)\right] + 1\right\} \\ & + \tfrac{1}{2} i\,(2\pi)^{-4} \int d^4k \left\{\ln\left[D'(k)/\bar{D}_0(k)\right] - \left[D'(k)/\bar{D}_0(k)\right] + 1\right\} \\ & + \sum_{\ell=2}^{\infty} f_\ell(D', S') \quad . \end{aligned} \tag{4.13}$$

The difference between $F(D', S')$ and $G(D', S')$ is

$$\begin{aligned} F - G = & \; U(\bar{\phi}) + (8\pi^3)^{-1} \int_F (2\kappa)\, d^3p\, (\vec{p}^{\,2} + m_0^2)^{\frac{1}{2}} \\ & - i\,(2\pi)^{-4} \int d^4p\ \text{trace}\left\{\ln\left[\bar{S}_0(p)/S_0(p)\right]\right\} \\ & + \tfrac{1}{2} i\,(2\pi)^{-4} \int d^4k \ln\left[\bar{D}_0(k)/D_0(k)\right] + \text{subtraction term} \quad . \end{aligned} \tag{4.14}$$

By using the identity

$$-i\,(2\pi)^{-1} \int_{-\infty}^{\infty} dk_0 \ln \frac{k^2 + \beta - i\epsilon}{k^2 + \alpha - i\epsilon} = (\vec{k}^{\,2} + \beta)^{\frac{1}{2}} - (\vec{k}^{\,2} + \alpha)^{\frac{1}{2}} \quad , \tag{4.15}$$

one finds

$$F - G = U(\bar{\phi}) + (8\pi^3)^{-1} \int_F (2\kappa)\, d^3p\, (\vec{p}^2 + \bar{m}_0^2)^{\frac{1}{2}}$$
$$- (8\pi^3)^{-1} \int (2\kappa)\, d^3p \left[(\vec{p}^2 + \bar{m}_0^2)^{\frac{1}{2}} - (\vec{p}^2 + m_0^2)^{\frac{1}{2}} \right]$$
$$+ \tfrac{1}{2} (8\pi^3)^{-1} \int d^3k \left[(\vec{k}^2 + \bar{a}_0)^{\frac{1}{2}} - (\vec{k}^2 + a_0)^{\frac{1}{2}} \right] + \text{subtraction term} \qquad (4.16)$$

where m_0 is given by (4.3), $a_0 = (1 + \delta Z_\phi)^{-1}(a + \delta a)$,

$$\bar{m}_0 = (1 + \delta Z_\psi)^{-1}(\bar{m} + \delta \bar{m}) \ ,$$

and

$$\bar{a}_0 = (1 + \delta Z_\phi)^{-1}(\bar{a} + \delta \bar{a}) \quad . \qquad (4.17)$$

Because $(F - G)$ is independent of D' and S', if one wishes, one may express the stationary conditions (4.9) and (4.10) in terms of G: $(\delta G/\delta D') = (\delta G/\delta S') = 0$. This leads to the same equations (4.11) and (4.12). We may substitute the iterative solutions of D' and S' back into G, and then express G as a sum of ℓ-loop diagrams ($\ell \geq 2$) in terms of $\bar{D}$ and $\bar{S}$. By comparing with the sum $\Sigma\, \mathcal{E}_{\ell\text{-loop}}$ in (3.21), we find that the difference between $\Sigma\, \mathcal{E}_{\ell\text{-loop}}$ and $G(D', S')$ is equal to the sum of all "one-loop" prototype diagrams which have only the counterterms $\delta\bar{m}$, $\delta\bar{a}$, δZ_ψ and δZ_ϕ as vertices. These diagrams are included in $\Sigma\, \mathcal{E}_{\ell\text{-loop}}$ but not in G. [See the discussion given after (3.21) in the previous section.] By using the identity (4.15), one finds that this difference is also equal to that between the righthand side of (4.16) and $\mathcal{E}_{q.cl.} + \Delta\mathcal{E}_{vac}$ [given by (3.19) and (3.20)]. Thus,

$$\mathcal{E}(n, \bar{\phi}) = F(D', S') \qquad (4.18)$$

where $\mathcal{E}(n, \bar{\phi})$ is given by (3.21). Theorem 2 is then proved.

From Theorem 1, one sees that F is also stationary with respect to $\bar{\phi}$. The physical value of $\bar{\phi}$ corresponds to a minimum of F.

B. Approximate Solutions

The variational formulation allows a convenient basis for making approximations.

1. As a first example, we may consider the simplest approximation in which all $f_\ell = 0$, but keeping $\bar{\phi} \neq 0$ in the definition of the functional F. From (4.11) and (4.12), one finds $D'(k) = \bar{D}_0(k)$ and $S'(p) = \bar{S}_0(p)$. It is clear that since in this approximation there is no (2-line irreducible) loop diagram in F, all counter terms should be zero; i.e., $\delta Z_\phi = \delta Z_\psi = \delta a = \delta b = \delta c = \delta m = \delta g = 0$. Therefore

$$D_0(k) = D(k) = -i\left[k^2 + a - i\epsilon\right]^{-1} ,$$

$$D'(k) = \bar{D}_0(k) = \bar{D}(k) = -i\left[k^2 + \bar{a} - i\epsilon\right]^{-1} ,$$

$$S_0(p) = S(p) = i\left[-i\gamma_\mu p_\mu - m + i\epsilon_n\right]^{-1} ,$$

and

$$S'(p) = \bar{S}_0(p) = \bar{S}(p) = i\left[-i\gamma_\mu p_\mu - \bar{m} + i\epsilon_n\right]^{-1} . \qquad (4.19)$$

After substituting these expressions into (4.2) and by using (4.15) and (4.18), one obtains

$$\mathcal{E}(n, \bar{\phi}) = \mathcal{E}_{q.cl.} + \Delta\mathcal{E}_{vac} \qquad (4.20)$$

where $\mathcal{E}_{q.cl.}$ and $\Delta\mathcal{E}_{vac}$ are given by (3.19) and (3.20) respectively. [Note that the identity (3.40) is not satisfied in this approximation.]

2. As a second example, we consider the approximation in which only the first two-loop diagram in Figure 6 is included; i.e., we set $f_\ell = 0$ for $\ell \geq 3$ and

$$-i f_2 = \tfrac{1}{2}(g+\delta g)^2 (2\pi)^{-8} \int d^4p\, d^4q\, D'(p-q)\ \text{trace}\left[S'(p)\, S'(q)\right] . \qquad (4.21)$$

Equations (4.11) and (4.12) become

$$\left[D'(k)\right]^{-1} - \left[\bar{D}(k)\right]^{-1} = -(g+\delta g)^2 (2\pi)^{-4} \int d^4p\ \text{trace}\left[S'(p)\, S'(p-k)\right] + i\left[(\delta Z_\phi)\, k^2 + \delta\bar{a}\right] \qquad (4.22)$$

and

$$\left[S'(p)\right]^{-1} - \left[\bar{S}(p)\right]^{-1} = (g+\delta g)^2 (2\pi)^{-4} \int d^4k\, D'(k)\, S'(p-k) - i\left[(\delta Z_\psi)(-i\gamma_\mu p_\mu) - \delta\bar{m}\right] \tag{4.23}$$

where $\bar{D}$ and $\bar{S}$ are given by (3.15) and (3.16) respectively. In these equations, $\bar{\phi}$ enters into the propagators $\bar{D}$ and $\bar{S}$ through

$$\bar{m} = m + g\bar{\phi} \quad \text{and} \quad \bar{a} = a + b\bar{\phi} + \tfrac{1}{2} c\bar{\phi}^2 .$$

We regard $\bar{\phi}$ as an independent parameter, and assume $g\bar{\phi} \sim O(m)$. Depending on the value of $\bar{\phi}$, $\bar{a}$ may be negative.

Let us discuss the solutions of these two coupled equations in the weak-coupling but high-density limit; i.e., we assume

$$\frac{g^2}{4\pi} \ll 1 \quad \text{and} \quad g^2 k_F^2 \sim O(a) \sim O(m^2) . \tag{4.24}$$

In this limit, just by power counting, one sees that the righthand side of (4.22) is typically $O(g^2 k_F^2)$, while that of (4.23) is $O(g^2 k_F) \ll m$. Thus, the zeroth-order solution of $S'(p)$ is $\bar{S}(p)$, and consequently (4.22) becomes

$$\left[D'(k)\right]^{-1} = \left[\bar{D}(k)\right]^{-1} - g^2 (2\pi)^{-4} \int d^4p \ \text{trace}\left[\bar{S}(p)\,\bar{S}(p-k)\right] + i\left[(\delta Z_\phi)\, k^2 + \delta a\right] , \tag{4.25}$$

since to this order $\delta g = \delta b = \delta c = 0$, and therefore $\delta\bar{a} = \delta a$. The solution is

$$D'(k) = -i\left[k^2 + \bar{a} + \Pi_{vac} + \Pi_F\right]^{-1} \tag{4.26}$$

where Π_{vac} is the usual vacuum-polarization correction to the renormalized mass operator of the meson field (in the absence of the Fermion density), and Π_F is due to the Fermion density.

It is not difficult to evaluate Π_F. We find

$$\Pi_F(\vec{k}^2, k_0) = \int_0^\infty (k_0^2 - E^2 + i\epsilon)^{-1} \left[-\rho_+(\vec{k}^2, E) + \rho_-(\vec{k}^2, E) \right] dE^2 \ , \quad (4.27)$$

$$\rho_+(\vec{k}^2, k_0) = g^2 \kappa (8\pi^3)^{-1} \int_F d^3q \, (\omega_q \omega_p)^{-1} (-2\bar{m}^2 + k_0 \omega_q - \vec{k} \cdot \vec{q}) \, \delta(k_0 - \omega_q - \omega_p) \quad (4.28)$$

and

$$\rho_-(\vec{k}^2, k_0) = g^2 \kappa (8\pi^3)^{-1} \int_F d^3q \, (\omega_q \omega_p)^{-1} (2\bar{m}^2 + k_0 \omega_q + \vec{k} \cdot \vec{q}) \, \delta(k_0 + \omega_q - \omega_p) \times \theta(|\vec{p}| - k_F) \ , \quad (4.29)$$

where $\theta(x)$ is a step-function, which is 1 if $x > 0$, and 0 if $x < 0$, $\omega_q = (\vec{q}^2 + \bar{m}^2)^{\frac{1}{2}}$ and $\vec{p} = \vec{k} - \vec{q}$. Both ρ_+ and ρ_- satisfy the positivity condition,

$$\rho_\pm(\vec{k}^2, E) \geqq 0 \ . \quad (4.30)$$

Because in (4.28) and (4.29) the integration extends only over $|\vec{q}| \leqq k_F$, one finds $\rho_\pm(\vec{k}^2, E) \neq 0$ only within a limited interval in E. The E-integration in (4.27) is, therefore, convergent. Physically, $-\rho_+$ is due to the "absence" of the pair-creation process into $N_{\vec{q}}$ and $\bar{N}_{\vec{p}}$ when $\vec{q}$ lies inside the Fermi sea (N denotes the Fermion and $\bar{N}$ the anti-Fermion), whereas ρ_- is due to the absorption process of converting a Fermion from $-\vec{q}$ in the Fermi sea to $\vec{p}$ out of the Fermi sea (as insured by the step-function θ). At $\vec{k} = 0$, one has

$$\rho_-(0, E) = 0 \ , \quad (4.31)$$

and

$$\rho_+(0, E) = \begin{cases} g^2 \kappa (8\pi^2 E)^{-1} (E^2 - 4\bar{m}^2)^{\frac{3}{2}} & \text{if } 2\omega_F > E > 0 \\ 0 & \text{otherwise} \end{cases} \quad (4.32)$$

where $\omega_F = (k_F^2 + \bar{m}^2)^{\frac{1}{2}}$. By using (4.27), one finds at $k_\mu = 0$

$$\Pi_F(0,\,0) \;=\; g^2\kappa(4\pi^3)^{-1}\int_F (\vec{q}^{\,2} + \bar{m}^2)^{-\frac{3}{2}}\,\vec{q}^{\,2}\,d^3q \quad . \tag{4.33}$$

In the high-density limit, (Π_{vac}/Π_F) is typically $\sim O(m^2/k_F^2) \ll 1$. Thus,

$$D'(k) \;\cong\; -\,i\left[k^2 + \bar{a} + \Pi_F\right]^{-1} . \tag{4.34}$$

If, in addition, we are interested in the region in which both $|\vec{k}|$ and k_0 are $\ll k_F$, then we have

$$D'(k) \;\cong\; -\,i\left[k^2 + \bar{a} + \Pi_F(0,\,0)\right]^{-1} \tag{4.35}$$

which, through (3.32) and for $\kappa = 2$, leads to the same expression as (3.36).

C. High-Density Weak-Coupling Expansion

We now turn to the case that (1.14) holds; i.e., $a \sim O(m^2) \sim O(g^2 k_F^2)$, $b^2 \sim O(ac)$ and $c \sim O(g^2) \ll 1$. Formally, one may expand in the form (1.15):

$$\mathcal{E}(n) \;=\; \mathcal{E}_0 + \mathcal{E}_1 + \mathcal{E}_2 + \cdots$$

where $\mathcal{E}_0 \sim O(k_F^4)$, $\mathcal{E}_1 \sim O(g^2 k_F^4)$ and $\mathcal{E}_2 \sim O(g^4 k_F^4)$, etc. In this case, neglecting higher-order corrections in g^2, one finds

$$S'(p) \;=\; \bar{S}(p) \;=\; i(-i\gamma_\mu p_\mu - \bar{m} + i\epsilon_n)^{-1} \tag{4.36}$$

but $D'(k)$ is given by (4.34), not $\bar{D}(k)$. Substituting these expressions into (4.2), one sees that there is only one two-loop diagram $\sim O(g^2 k_F^4)$, and that is the first two-loop diagram in Figure 6. By using (4.34), (4.36) and the result derived in Appendix C, we find that to $O(g^2 k_F^4)$, the sum over all loop diagrams is given by (3.41), or (3.42). Therefore, in the case of a single ϕ field, to $O(g^2 k_F^4)$ the energy-density function is given by (1.17). In the case of the σ-model, because of pion-exchanges, we have, instead of (1.17),

$$\mathcal{E} = \tfrac{1}{4}\lambda^2(\bar{\sigma}^2 - \sigma_0^2)^2 + (2\pi^3)^{-1}\int d^3p\,(\vec{p}^2 + g^2\bar{\sigma}^2)^{\frac{1}{2}} - (16\pi^2)^{-1} g^2 k_F^4 \quad . \tag{4.37}$$

In either case, we derive the same expression for the dependence of $m_{eff}^2 = (m + g\bar{\phi})^2$, or $(g\bar{\sigma})^2$, on the Fermion density as that given by the quasi-classical solution.

The evaluation of the next order $O(g^4 k_F^4)$ term is straightforward but complicated. The details will be given in a separate publication.

V. Remarks

From the above discussion, it is clear that, at least when the expansion (1. 15) is valid, the general character of the quasi-classical solution remains correct with the inclusion of quantum corrections. For physical applications to the abnormal nuclear states, the parameter $(4\pi)^{-1} g^2$ is, in general, not a small one. Nevertheless, as already remarked in the Introduction, since the shift of $\bar{\phi}$, from its normal value 0 to the abnormal value $-(m/g)$, is smallest in the strong-coupling limit[12], so also may be the difference between the quantum correction in the abnormal state and that in the vacuum state. On the other hand, the lack of information concerning the vacuum state itself makes it difficult to perform calculations in the strong-coupling limit.

There is a certain analogy between the abnormal state and the Bose-Einstein condensation. Mathematically, the Bose-Einstein transition can be rigorously treated only for ideal Bosons and for Bosons with either weak interactions or small scattering lengths. For physical applications, He^4 is known to have strong interactions; yet, it does undergo Bose-Einstein condensation and exhibits superfluidity. Through the B. C. S. pair-correlation, the electrons in metals exhibit similar phase transitions that give rise to superconductivity. Recently, it has been observed that even He^3 exhibits superfluidity. Likewise, it seems reasonable to expect that the transition to the abnormal state is a fairly general phenomenon, not restricted to the validity of the particular expansion (1. 15).

One of us (T. D. L.) wishes to thank G. C. Wick and A. Kerman for discussions.

Appendix A

In this appendix, we examine the temperature effect on the system at low temperature. Let

$$\theta = \text{Boltzmann constant} \times \text{absolute temperature} . \tag{A.1}$$

We assume the temperature to be sufficiently low, $\theta \ll k_F$ and $a^{\frac{1}{2}}$, so that the Fermions remain degenerate and there are no free mesons. In the quasi-classical treatment, in which ϕ is assumed to be constant, the Helmholtz free energy F is given by

$$\Omega^{-1} F = nkT \ln z + U(\phi) - \pi^{-2} \kappa \theta \int_0^\infty k^2 \, dk \ln \left[1 + z e^{-\omega/\theta} \right] \tag{A.2}$$

where $U(\phi)$ and κ are given by (1.2) and (1.9) respectively,

$$\omega = \left[k^2 + (m + g\phi)^2 \right]^{\frac{1}{2}} \tag{A.3}$$

and z is the fugacity, related to the Gibbs thermodynamic potential μ per Fermion by

$$z = \exp(\mu/\theta) . \tag{A.4}$$

The average number of Fermions with wave number k (and at a given spin and, say, isospin state) is

$$n_k = \left[z^{-1} \exp(\omega/\theta) + 1 \right]^{-1} , \tag{A.5}$$

and the Fermion density is

$$n = \pi^{-2} \kappa \int k^2 \, dk \, n_k . \tag{A.6}$$

The physical value of ϕ is determined by the minimum of $\Omega^{-1} F$, keeping n and θ fixed.

At low temperature, by using (A.2)-(A.6), we find

$$\Omega^{-1}F = U(\phi) + \pi^{-2}\kappa \int_0^{k_F} q^2 \omega \, dq - \frac{1}{6}\kappa\theta^2 k_F \omega_F + O(\theta^4) \qquad (A.7)$$

where

$$k_F \equiv (3\pi^2 n/\kappa)^{\frac{1}{3}} \qquad (A.8)$$

and

$$\omega_F = \left[k_F^2 + (m+g\phi)^2\right]^{\frac{1}{2}} . \qquad (A.9)$$

For the σ-model interacting with a nucleon field, (A.7) becomes

$$\Omega^{-1}F = \frac{\lambda^2}{4}(\sigma_0^2 - \sigma^2)^2 + \frac{2}{\pi^2}\int_0^{k_F} q^2 \omega \, dq - \tfrac{1}{3}\theta^2 k_F \omega_F + O(\theta^4) \qquad (A.10)$$

where

$$\omega = \left[q^2 + (g\sigma)^2\right]^{\frac{1}{2}} \quad \text{and} \quad \omega_F = \left[k_F^2 + (g\sigma)^2\right]^{\frac{1}{2}} .$$

Let us consider the special case that at zero temperature the abnormal state (i.e., $\sigma = 0$) is stable; according to (2.19), one has

$$\frac{g^2}{4\pi} > \frac{3\pi}{16}\left(\frac{m_\sigma}{m_N}\right)^2 . \qquad (A.11)$$

The density of the abnormal state at zero temperature is given by (2.20):

$$n_{Ab} = (2\pi\sqrt{3})^{-\frac{1}{2}}(m_N m_\sigma/g)^{\frac{3}{2}} . \qquad (A.12)$$

From (A.10), one sees that for $\theta \ll k_F$, and at density $n > n_{Ab}$, the minimum of F remains given by $\sigma = 0$; i.e., for the abnormal phase

$$\Omega^{-1} F = \frac{m_\sigma^2 m_N^2}{8g^2} + \frac{k_F^4}{2\pi^2} - \frac{1}{3}\theta^2 k_F^2 + O(\theta^4) \quad . \tag{A. 13}$$

The corresponding thermodynamic pressure p is [after neglecting $O(\theta^4)$]

$$p = \frac{1}{4}\left(\frac{3\pi^2}{2}\right)^{\frac{1}{3}} (n^{\frac{4}{3}} - n_{Ab}^{\frac{4}{3}}) + \frac{1}{9}\left(\frac{3\pi^2}{2}\right)^{\frac{2}{3}} \theta^2 n^{\frac{2}{3}} \quad . \tag{A. 14}$$

When $n < n_{Ab}$, as the density decreases, because of evaporation the system no longer stays in a single abnormal phase. In the two-phase region, we may define the "liquid phase" to be the abnormal state $(\sigma = 0)$, while the "gas phase" is the normal state $(\sigma = \sigma_0)$; in the gas phase the nucleons form a nondegenerate gas. Because of the low density, the gas phase can be approximately described by the perfect gas law. By equating the fugacities in these two phases, one finds that in the two-phase region p is given approximately by

$$p = 4\theta \left(\frac{m_N \theta}{2\pi}\right)^{\frac{3}{2}} e^{-(u/\theta)} \tag{A. 15}$$

where u is the binding energy per nucleon in the abnormal state; i.e., according to (2. 18),

$$u = m_N - k_F \cong m_N \left[1 - \left(\frac{3\pi^2 m_\sigma^2}{4g^2 m_N^2}\right)^{\frac{1}{4}}\right] \quad . \tag{A. 16}$$

Let v_g and v_ℓ be, respectively, the specific volumes in the gas and liquid phases in the two-phase region. From the perfect gas law, v_g is related to the pressure p by

$$v_g = p^{-1}\theta \quad , \tag{A. 17}$$

and from (A. 14), v_ℓ is related to the same p by

$$v_\ell \cong v_0 \left[1 + \frac{\pi^2}{2} \left(\frac{\theta}{k_0} \right)^2 - \frac{9\pi^2}{2} \frac{p}{k_0^4} \right] \qquad \text{(A. 18)}$$

where v_0 and k_0 are the specific volume and the Fermi momentum in the abnormal state at zero temperature; i.e.,

$$v_0 = n_{Ab}^{-1} = (2\pi\sqrt{3})^{\frac{1}{2}} (m_N m_\sigma / g)^{-\frac{3}{2}} \qquad \text{(A.19)}$$

and

$$k_0 = (3\pi^2 n_{Ab}/2)^{\frac{1}{3}} \ . \qquad \text{(A.20)}$$

See Figure 4 (case i) for a plot of the two-phase region.

Appendix B

We discuss here a simplified "hard sphere" model. Let us consider a nuclear medium of density n, and define r by

$$n^{-1} = \frac{4\pi}{3} r^3 \quad . \tag{B.1}$$

For free nucleons, the top Fermi momentum is related to r by the usual expression (for $\kappa = 2$)

$$k_F = \tfrac{1}{2}(9\pi)^{\frac{1}{3}} / r \quad . \tag{B.2}$$

Because of the short-range repulsive force between nucleons, the average de Broglie wavelength of each nucleon would be shorter than that in the free case; consequently, the nuclear momentum should be correspondingly increased. Nevertheless, phenomenologically we may still regard the nucleons to form a degenerate Fermi sea, but with its top Fermi momentum raised from k_F to [13]

$$K_F \equiv \tfrac{1}{2}(9\pi)^{\frac{1}{3}} / (r - 0.8\,d) \tag{B.3}$$

where d is a phenomenological parameter. The average kinetic energy per nucleon is then given by

$$u_N = \frac{\int_0^{K_F} k^2 (k^2 + m_{eff}^2)^{\frac{1}{2}}\, dk}{\int_0^{K_F} k^2\, dk}$$

or,

$$u_N = \tfrac{3}{4} K_F \left\{ (1+x^2)^{\frac{1}{2}} (1 + \tfrac{1}{2}x^2) - \tfrac{1}{2} x^4 \ln \left[x^{-1} + (x^{-2}+1)^{\frac{1}{2}} \right] \right\} \tag{B.4}$$

where $x = m_{eff}/K_F$ and m_{eff} is given by (1.7). The combination $0.8\,d$ in (B.3) is

chosen such that for a system of hard spheres, in the dilute (therefore also non-relativistic) limit, (B.4) gives the exact energy expression to $O(n^{\frac{1}{3}} d)$, provided[13]

$$d = \text{diameter of the hard sphere} . \tag{B.5}$$

In addition to u_N, there is also the potential energy $U(\phi)$ of the spin 0 field. In the quasi-classical approximation, the total energy $E \equiv \Omega \mathcal{E}$ of the system is given by

$$A^{-1} E \cong u_N + n^{-1} U(\phi) \tag{B.6}$$

where A is the total nucleon number.

1. Abnormal state

In (B.6), except through the average ϕ field, all other effects due to the usual short-range attractive force between nucleons are not included. Such an approximation may not be too unreasonable (though definitely crude) for the abnormal state, since the basic energy scale there is rather large $\sim O(m_N)$. In the abnormal state, we may set $\phi \cong -(m/g)$; therefore $m_{eff} \cong 0$ and

$$A^{-1} E \cong \tfrac{3}{4} K_F + n^{-1} U_0 \tag{B.7}$$

where

$$U_0 \equiv U(\phi) \quad \text{at} \quad \phi = -(m/g) . \tag{B.8}$$

By varying the volume Ω at a fixed A, we find that the minimum E occurs at

$$r(r - .8d) = \tfrac{1}{4} \left(\frac{3}{2U_0}\right)^{\frac{1}{2}} \left(\frac{3}{\pi}\right)^{\frac{1}{3}} , \tag{B.9}$$

and its value is

$$A^{-1} E_{min} \cong K_F \left[1 + \tfrac{1}{5} (r - .8\, d)^{-1} d \right] . \qquad \text{(B. 10)}$$

In the σ-model, $U_0 = (8g^2)^{-1} m_\sigma^2 m_N^2$. As an illustration, in Figure 8 the binding energy per nucleon

$$u \equiv m_N - A^{-1} E_{min} \qquad \text{(B. 11)}$$

is plotted versus d for $m_\sigma = 700$ MeV and $(4\pi)^{-1} g^2 = 5$ and 10. We may take, as a further example, $d = 2/m_\omega \cong .5$ fm where m_ω is the mass of the ω^o-meson; for $m_\sigma = 700$ MeV and $(4\pi)^{-1} g^2 = 5$, we find $r \cong .86$ fm, $n^{-1} U_0 \cong 300$ MeV, $\frac{3}{4} K_F \cong 490$ MeV and therefore the binding energy $u \cong 150$ MeV per nucleon.

2. Normal state

If the σ-model is to be regarded as an approximation to reality, then the normal nuclear state should appear as a minimum, either local or absolute, of the (volume) energy E. Thus, it is of interest to search for the condition that E has two minima: one for the normal state ($\sigma \cong \sigma_0$) and the other for the abnormal state ($\sigma \cong 0$). On the other hand, in the normal state, the usual short-range attractive force between nucleons should be important. Thus, (B.6) is not expected to be a reasonable approximation[14]. Nevertheless, purely as a mathematical model, one may ask under what condition does E, given by (B.6), have two minima? By using (2. 11) and (2. 14), one sees that in the σ-model, (B.6) may be written as (after requiring $\vec{\pi} = 0$)

$$A^{-1} E \cong u_N + (8g^2 n)^{-1} m_\sigma^2 m_N^2 (y^2 - 1)^2 \qquad \text{(B. 12)}$$

where $y = \sigma/\sigma_0$, u_N is given by (B.4) with $x = | y m_N / K_F |$. Set $m_N = 940$ MeV;

$A^{-1}E$ depends only on two parameters: $(m_\sigma/g)^2$ and d. By varying $A^{-1}E$ with respect to σ and r, we may search for its minima. In Figure 9, we map out the region in which $A^{-1}E$ has two minima, and both minima have a positive binding energy. The region turns out to be extremely narrow, because of the requirement that there also be a "bound" normal state in this simple model.

Appendix C

In Figure 6, we see that there are only three two-loop diagrams, apart from other related diagrams which involve counter terms. Among these three diagrams, the second and the third diagrams have been evaluated in Ref. 1. [See Eq. (3.17) of Ref. 1.] In this Appendix, we discuss only the first two-loop diagram, hereafter referred to as $\mathcal{G}$, in Figure 6.

1. Prototype Diagram (a single 0+ Boson field)

Let us first consider the case that $\mathcal{G}$ is a prototype diagram and there is only a single 0+ Boson field besides the Fermions. Its contribution to the energy density is (also denoted by $\mathcal{G}$, for simplicity)

$$\mathcal{G} = \tfrac{1}{2} i g^2 (2\pi)^{-8} \text{ trace } \int d^4p\, d^4q\, \bar{D}(p-q)\ \bar{S}(p)\ \bar{S}(q) \qquad \text{(C. 1)}$$

where $\bar{D}$ is given by (3.15) and $\bar{S}$ by (3.16). The p_0- and q_0-integrations can be carried out by converting their contours from the real axes to those around the cuts in their respective upper-half planes. In either the p_0- or q_0-complex plane, immediately above the real axis there are two such cuts: one is from $|\bar{m}|$ to $(k_F^2 + \bar{m}^2)^{\frac{1}{2}}$ due to the positive-energy Fermi sea, and the other is from $-\infty$ to $-|\bar{m}|$ due to the negative-energy Dirac sea, where $\bar{m}$ is given by (3.12). Thus, (C. 1) can be written as

$$\mathcal{G} = \mathcal{G}_{++} + \mathcal{G}_{+-} + \mathcal{G}_{--} \qquad \text{(C. 2)}$$

where $\mathcal{G}_{++}$ (or $\mathcal{G}_{--}$) is due entirely to the positive (or negative) energy-cuts in both the p_0- and q_0-planes, while $\mathcal{G}_{+-}$ is due to the positive energy-cut in one plane and the negative energy-cut in the other. It is easy to see that at high density,

$\mathcal{L}_{++} \sim O(g^2 k_F^4)$, $\mathcal{L}_{+-} \sim O(g^2 k_F^2 m^2)$ and $\mathcal{L}_{--} \sim O(g^2 m^4)$. Thus to $O(g^2 k_F^4)$, only $\mathcal{L}_{++}$ is of importance; i.e., $\mathcal{L}$ is dominated by

$$\mathcal{L}_{++} = \tfrac{1}{2} g^2 \kappa (2\pi)^{-6} \int_F d^3p\, d^3q \left[(p-q)^2 + \bar{a}\right]^{-1} (\vec{p}^2 + \bar{m}^2)^{-\frac{1}{2}} (\vec{q}^2 + \bar{m}^2)^{-\frac{1}{2}} \times \left[\tfrac{1}{2}(p-q)^2 + 2\bar{m}^2\right] \qquad (C.3)$$

in which both $\vec{p}$ and $\vec{q}$ lie inside the Fermi sea. The dominant contribution in (C.3) is due to $\vec{p}^2 \sim O(k_F^2)$, $\vec{q}^2 \sim O(k_F^2)$ and $(p-q)^2 \sim O(k_F^2)$. Thus, we have

$$\mathcal{L} \cong \mathcal{L}_{++} = (64\pi^4)^{-1} \kappa g^2 k_F^4 + O\left[g^2 k_F^2 m^2 \ln(k_F/m)\right] . \qquad (C.4)$$

The physical origin of the above $O(g^2 k_F^4)$ term can be understood by first calculating the self-energy change ΔE_p for a Fermion of momentum $\vec{p}$ in the presence of a Fermi sea (because of the exclusion principle). One can readily verify that for $k_F \gg \bar{m}$ and $\bar{a}^{\frac{1}{2}}$,

$$\Delta E_p \cong (16\pi^2)^{-1} g^2 k_F^2 (\vec{p}^2 + \bar{m}^2)^{-\frac{1}{2}}$$

which leads to an energy-density change of an amount

$$(8\pi^3)^{-1} 2\kappa \int_F d^3\vec{p} (\tfrac{1}{2} \Delta E_p) \cong (64\pi^4)^{-1} \kappa g^2 k_F^4 . \qquad (C.5)$$

To derive the lower order-expression in k_F^2, the integral (C.3) should be evaluated exactly. We find

$$\mathcal{L}_{++} = (4\pi)^{-4} \kappa g^2 \bar{m}^4 \left[(\sinh\omega - \omega)^2 + (1 - \tfrac{1}{2}\lambda) f\right] \qquad (C.6)$$

where

$$f = 32\int_0^{\omega/2} d\theta \sinh\theta \left\{(\lambda\cosh\theta)\ln\left[\lambda^{-1}(\cosh 2\theta + \lambda - 1)\right] - 2\theta(\lambda-1)\sinh\theta + 2\lambda(\lambda-2)(\csc A \sinh\theta)\tan^{-1}(\tanh\theta \tan\frac{A}{2})\right\}, \tag{C.7}$$

$\omega = 2\sinh^{-1}(k_F/\bar{m})$, $\lambda = \frac{1}{2}\bar{a}/\bar{m}^2$ and $\cos A = \lambda - 1$. In the high-density limit, $\omega \gg 1$; thus, $f \sim 2\omega^2 e^{\omega}$ and consequently $\mathcal{G}_{++} \sim (4\pi)^{-4}\kappa g^2 \bar{m}^4 \sinh^2\omega \sim 4(4\pi)^{-4}\kappa g^2 k_F^4$, which agrees with (C.4). We have also evaluated the other two terms $\mathcal{G}_{+-}$ and $\mathcal{G}_{--}$ in (C.2). The calculation is tedious though straightforward. The final expression is quite long; it will be given in a separate publication.

2. Prototype diagram (σ-model)

Next, we consider the σ-model in which there is the $\vec{\pi}$ field, besides the 0+ σ-field. Instead of (C.4), we find (after setting $\kappa = 2$ and summing over both σ-exchange and $\vec{\pi}$-exchange)

$$\mathcal{G} \cong \mathcal{G}_{++} = -(16\pi^4)^{-1} g^2 k_F^4 + O\left[g^2 k_F^2 m^2 \ln(k_F/m)\right] . \tag{C.8}$$

Since, in Figure 6, according to Eq. (3.17) of Ref. 1, except for $\mathcal{G}$ the other two diagrams are both $\sim O(a^2)$; from (C.4) and (C.8) we derive (3.41) and (3.42).

3. Two-line irreducible diagram

Lastly, we assume the diagram $\mathcal{G}$ to be a two-line irreducible diagram. According to the rules given in Section IV, instead of (C.1) we have

$$\mathcal{G} = \tfrac{1}{2} i g^2 (2\pi)^{-8} \text{ trace } \int d^4p\, d^4q\, D'(p-q)\, S'(p)\, S'(q) . \tag{C.9}$$

By using (4.27), (4.34) and (4.36), we find that (C.4) remains valid if there is only a single 0+ meson field, and that (C.8) remains valid if there is, in addition, also the $\vec{\pi}$-field. Thus, (1.17) and (4.37) are both established.

References

1. T. D. Lee and G. C. Wick, Phys. Rev. D9, 2291 (1974).
2. See also a talk given by T. D. Lee at the Annual Bevatron Users Meeting, Lawrence Berkeley Laboratory, January 1974 [Columbia University preprint CO-2271-27].
3. A preliminary report of this work was given by T. D. Lee at the XVII International Conference on High Energy Physics, London, July 1974 [Columbia University preprint CO-2271-39].
4. For references on the σ-model, see B. W. Lee, Chiral Dynamics (Gordon and Breach, 1972).
5. W. Thirring, Ann. Phys. 3, 91 (1958). See also J. M. Luttinger, J. Math. Phys. 4, 1154 (1963), and D. C. Mattis and E. H. Lieb, J. Math. Phys. 6, 304 (1965).
6. T. D. Lee and C. N. Yang, Phys. Rev. 117, 22 (1960).
7. S. Coleman and E. Weinberg, Phys. Rev. D7, 1888 (1973).
8. See, e.g., the review article by G. Kramer, Springer Tracts in Modern Physics 55, 158 (1970); the review article by the Particle Data Group in Rev. Mod. Phys. 45, no. 2, part II (1973), and also the article by S. Protopopescu et al. in Experimental Meson Spectroscopy - 1972, edited by A. H. Rosenfeld and K.-W. Lai (A. I. P., New York, 1972).
9. See S. Weinberg, Phys. Rev. D9, 3357 (1974); L. Dolan and R. Jackiw, Phys. Rev. D9, 3320 (1974).
10. V. M. Galitskii and A. B. Migdal, Soviet Physics, JETP 7, 96 (1958).
11. In the absence of the spin $\frac{1}{2}$ field, Eqs. (3.27) and (3.28) of this paper reduce to Eq. (3.8) of Ref. 1 through the relation $\bar{a} = a(1 + \Delta)$.

12. As $g \to \infty$, both the shift $\bar{\phi} = -(m/g)$ and the critical density approach zero. In this connection, see also some related work on quark models by W. A. Bardeen, M. S. Chanowitz, S. D. Drell, M. Weinstein and T. M. Yan [SLAC preprint-1490 (1974)], and M. Creutz [Brookhaven preprint BNL 18789 (1974)]. Cf. also P. Vinciarelli, Lettere al Nuovo Cimento 4, 905 (1972).

13. See e.g., A. Bohr and B. R. Mottelson, Nuclear Structure, vol. 1 (W. A. Benjamin, Inc., New York, 1969), p. 256.

14. In the normal state, if $U(\phi)$ is replaced by its quadratic approximation, $U(\phi) \cong \frac{1}{2} a \phi^2$, then (B.6) does give a surprisingly good fit to many of the properties of the existing nuclei. For details, see the Appendix of Ref. 2, and also R. Serber (to be published).

CAPTIONS

Figure 1. Examples of (i) a discontinuous transition and (ii) a continuous transition between the normal state ($m_{eff} \cong$ free Fermion mass m) and the abnormal state ($m_{eff} \cong 0$). The necessary conditions for a discontinous transition (i.e., case i) are $b^2 > 2ac$ and b of the same sign as g; both conditions are satisfied in the σ-model. In case ii, the function $U(\phi)$ can have either two minima (solid curve), or only one minimum (dashed curve).

Figure 2. Schematic drawings of $dU_\phi/d\phi$ and $-(\partial U_F/\partial\phi)_n$ versus ϕ for the cases (i)-(iv) discussed in Section II A.

Figure 3. The solid curve denotes $n_c = 2n_0$ where $n_0 = \left[\frac{1}{3}4\pi(1.2\text{ fm})\right]^{-1}$ and n_c is the critical density in the σ-model. Over a fairly wide range of m_σ and g, $n_c \cong 11.6\,(m_\sigma/m_N)^2\,(4\pi/g^2)\,n_0$.

Figure 4. $p - v$ diagram in the σ-model. θ = Boltzmann constant times the absolute temperature, p = pressure, v = specific volume and v_0 is given by (A. 19). Case (i) is for $(4\pi)^{-1} g^2 > (16)^{-1} 3\pi (m_\sigma/m_N)^2$: at $\theta = 0$, the transition occurs at $p = 0$. The graph is plotted for a choice of parameters such that the binding energy $u = 100$ MeV per Fermion in the abnormal state (i.e., liquid phase). Case (ii) is for $(4\pi)^{-1} g^2 < (16)^{-1} 3\pi (m_\sigma/m_N)^2$: at $\theta = 0$ the transition occurs at $p > 0$.

Figure 5. Graphical representation of the usual perturbation-series expansion of $\bar{\phi}$ and $\mathcal{E}(n)$.

Figure 6. $\mathcal{E}_{\ell\text{-loop}}$ in terms of prototype diagrams for $\ell = 2$ and 3. The symmetry number of each diagram is listed under the diagram. In the case of $\ell = 2$, there are only three prototype diagrams (except for diagrams involving counter terms which are represented by $\cdots$).

Figure 7. $U(\bar{\sigma})$, $\Delta\mathcal{E}_{vac}$ and $\Delta\mathcal{E}'_{vac}$ in units of $(8g^2)^{-1} m_\sigma^2 m_N^2$ versus $(\bar{\sigma}/\sigma_0)$. In this unit, $U(\bar{\sigma}) = \left[1 - (\bar{\sigma}/\sigma_0)^2\right]^2$, shown by the solid curve. The dotted curve denotes $\Delta\mathcal{E}_{vac}$ [Eq. (3.31)], and the dashed curve denotes $\Delta\mathcal{E}'_{vac}$ [Eq. (3.35)]; the latter is plotted for $n = 6n_0$, where $n_0^{-1} = \frac{1}{3} 4\pi (1.2\ \text{fm})^3$.

Figure 8. Binding energy per nucleon u versus diameter d of the hard-sphere repulsion for $m_\sigma = 700$ MeV and $(4\pi)^{-1} g^2 = 5$ and 10. Notice that, because of (B.9)-(B.11), u depends only on two unknown parameters: d and the ratio $(m_\sigma/g)^2$.

Figure 9. The region in which $A^{-1} E$, given by (B.12) in the simplified "hard sphere" model, has two minima, and both minima have a positive binding energy. One of the minima corresponds to the normal state ($\sigma \cong \sigma_0$) and the other to the abnormal state ($\sigma = 0$).

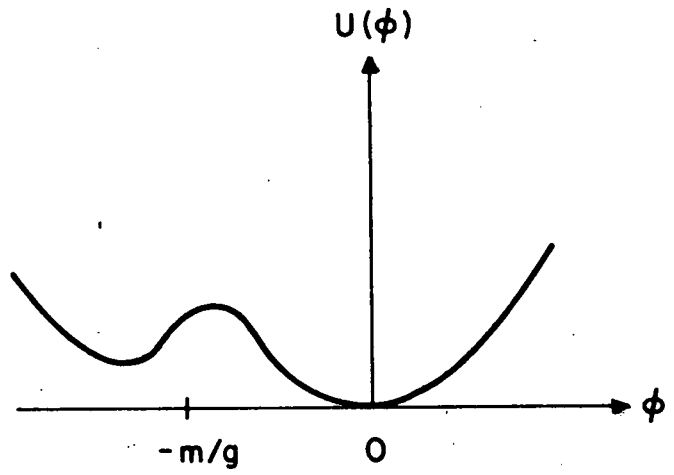

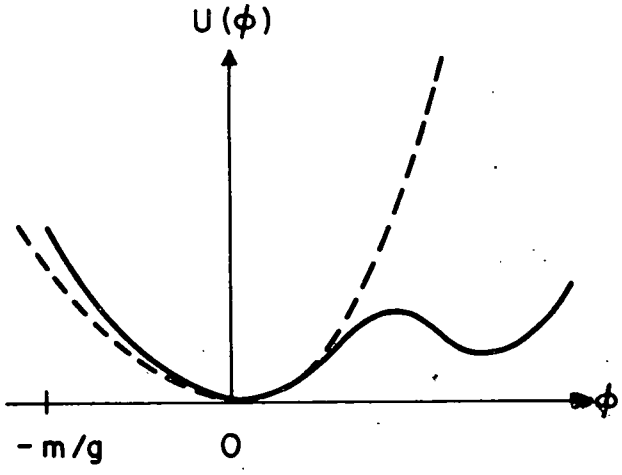

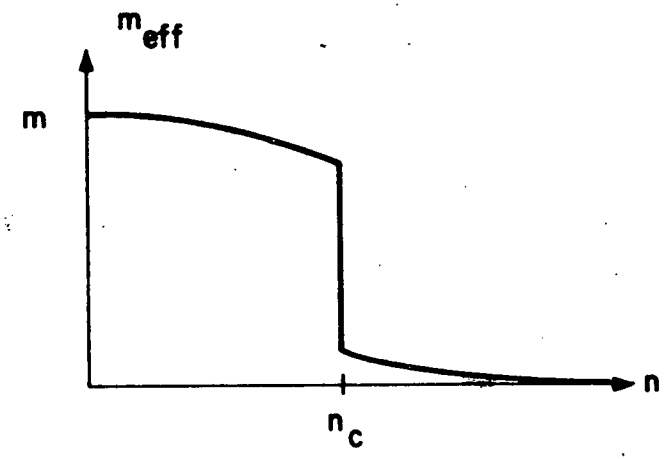

(i)

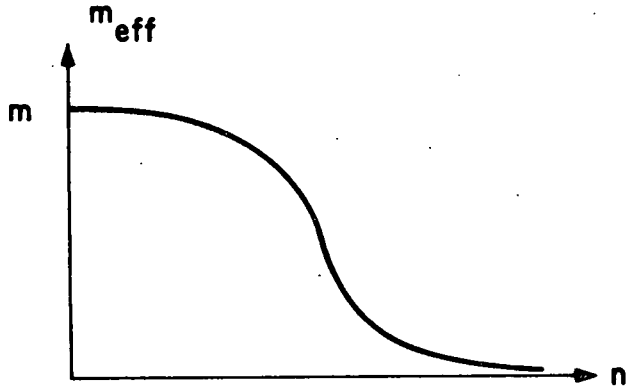

(ii)

Figure 1

Dashed Curve : $-\left(\frac{\partial U_F}{\partial \phi}\right)_n$

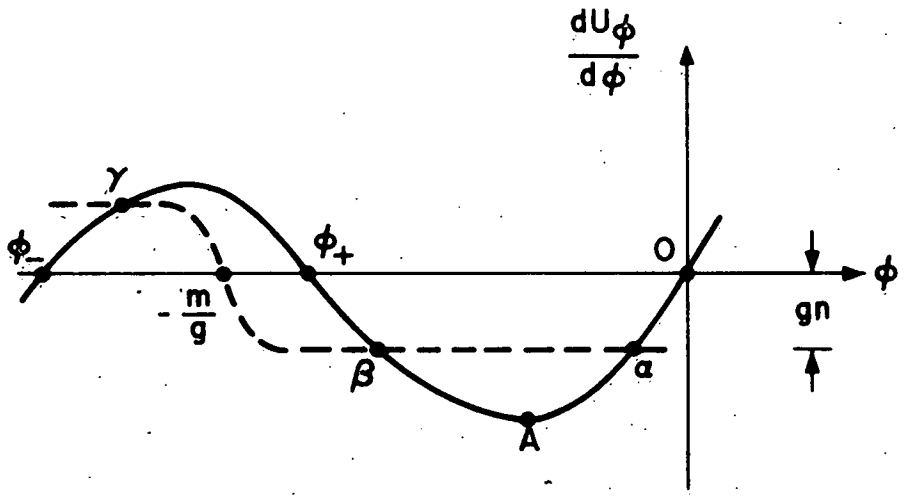

(i)

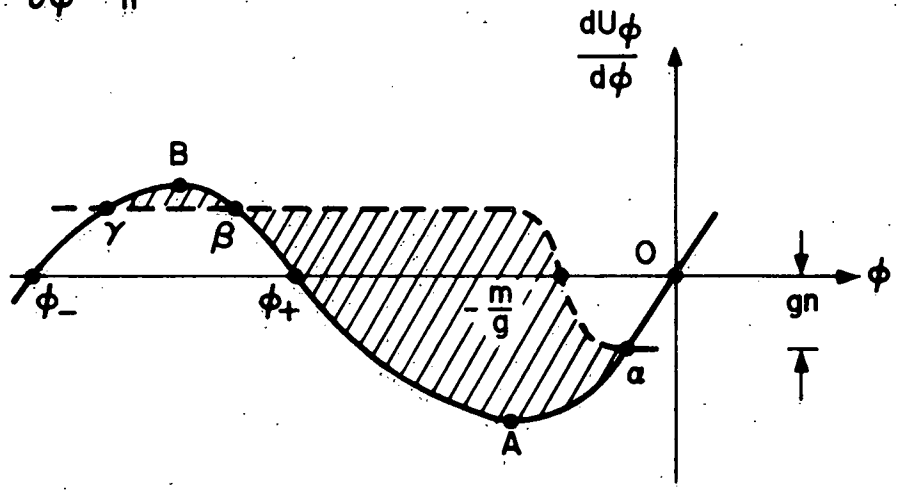

(ii)

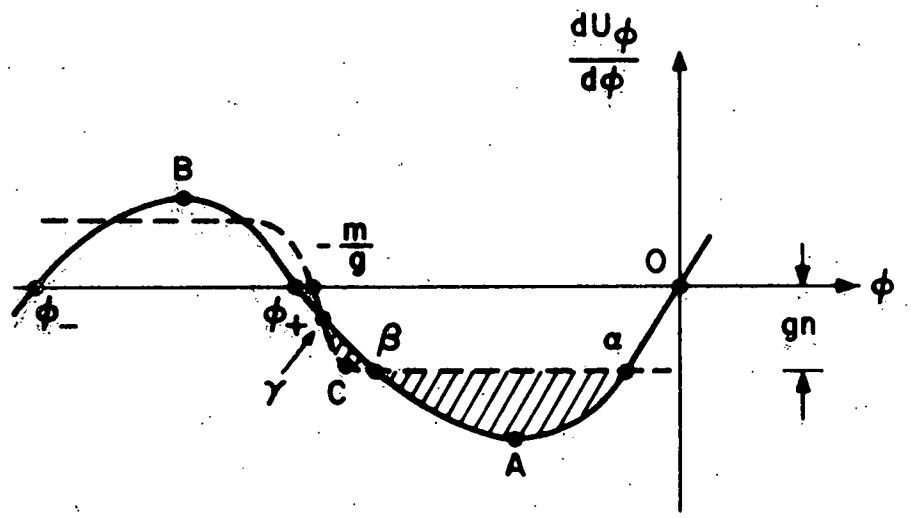

(iii)

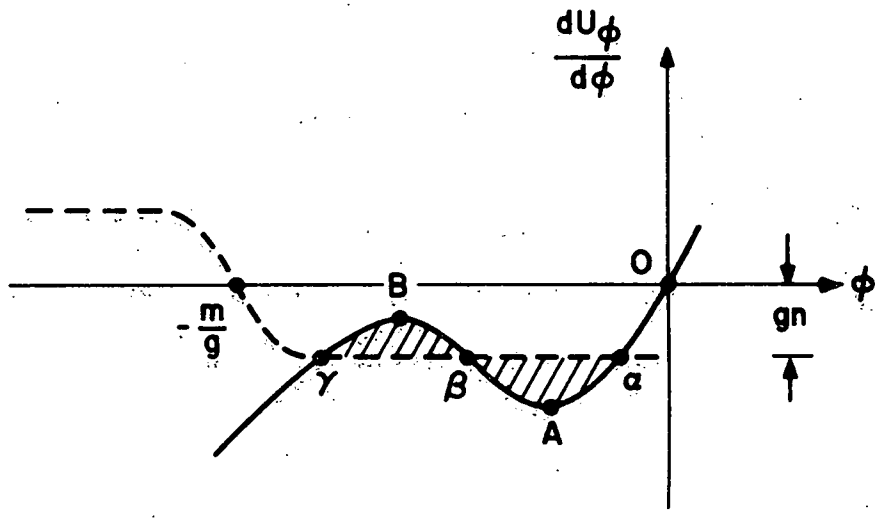

(iv)

Figure 2

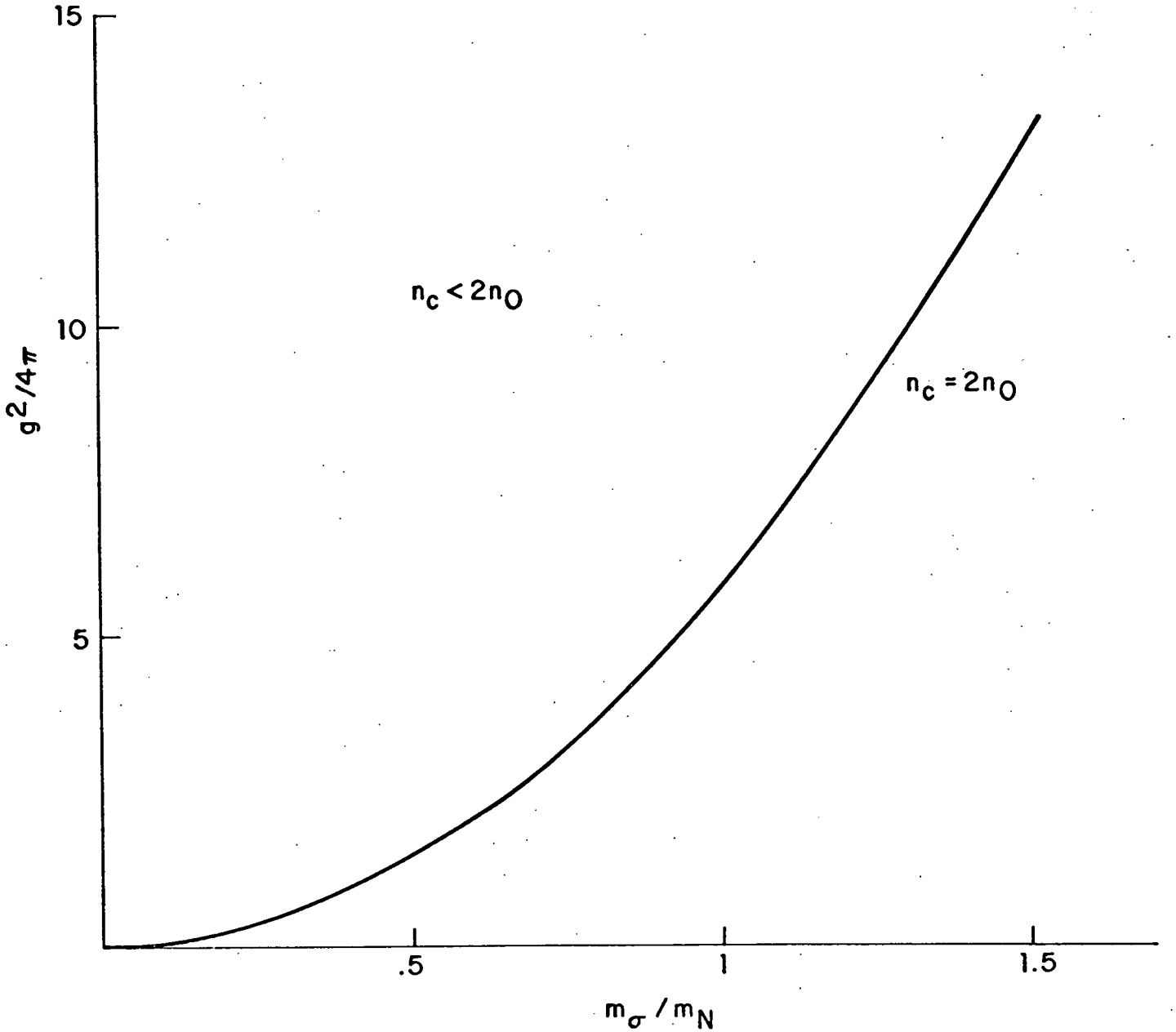

Figure 3

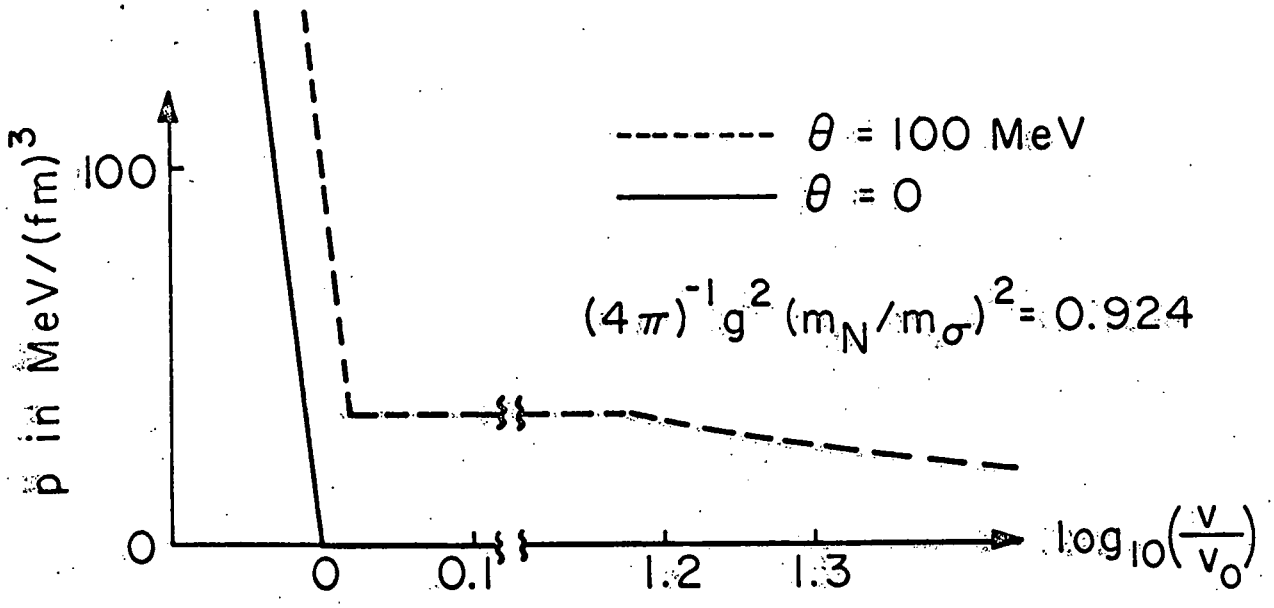
p in MeV/(fm)^3
100
0
θ = 100 MeV
θ = 0
$(4\pi)^{-1} g^2 (m_N/m_\sigma)^2 = 0.924$
0
0
0.1
1.2
1.3
$\log_{10}\left(\frac{v}{v_0}\right)$

(i)

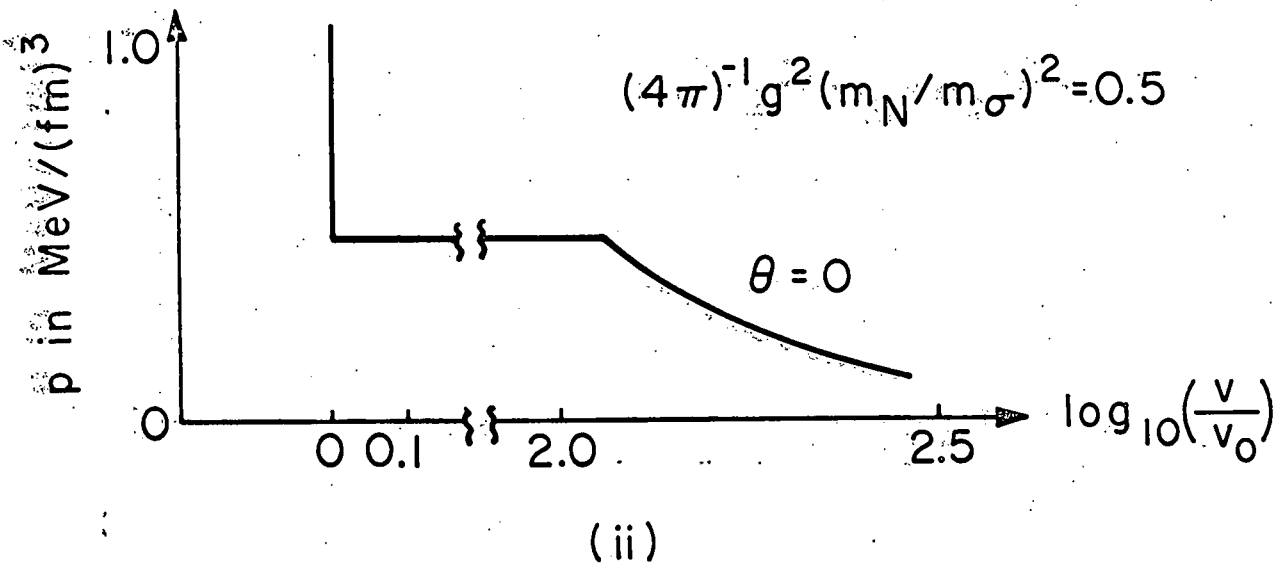
p in MeV/(fm)^3
1.0
0
$(4\pi)^{-1} g^2 (m_N/m_\sigma)^2 = 0.5$
θ = 0
0 0.1
2.0
2.5
$\log_{10}\left(\frac{v}{v_0}\right)$

(ii)

Figure 4

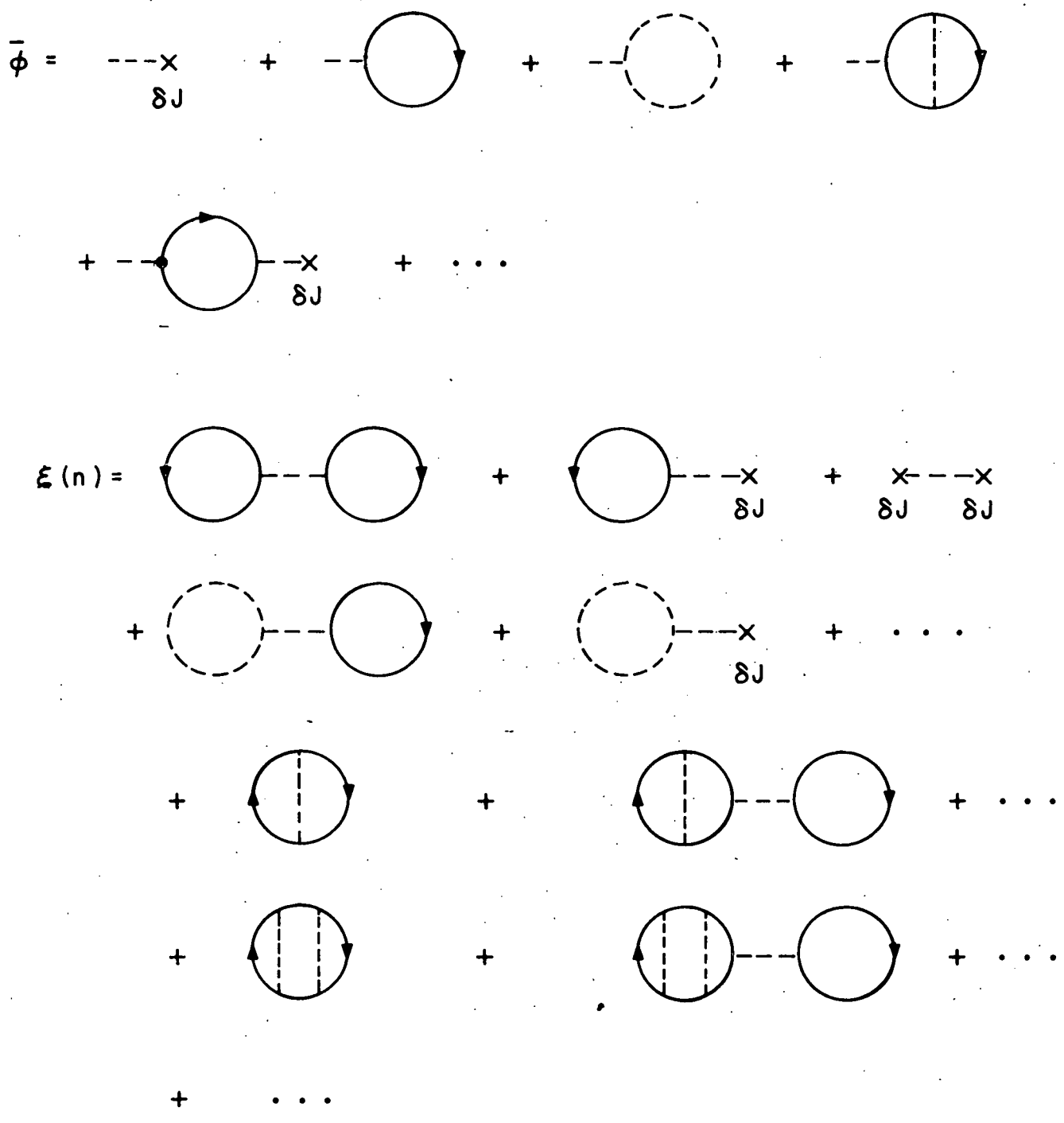

Figure 5

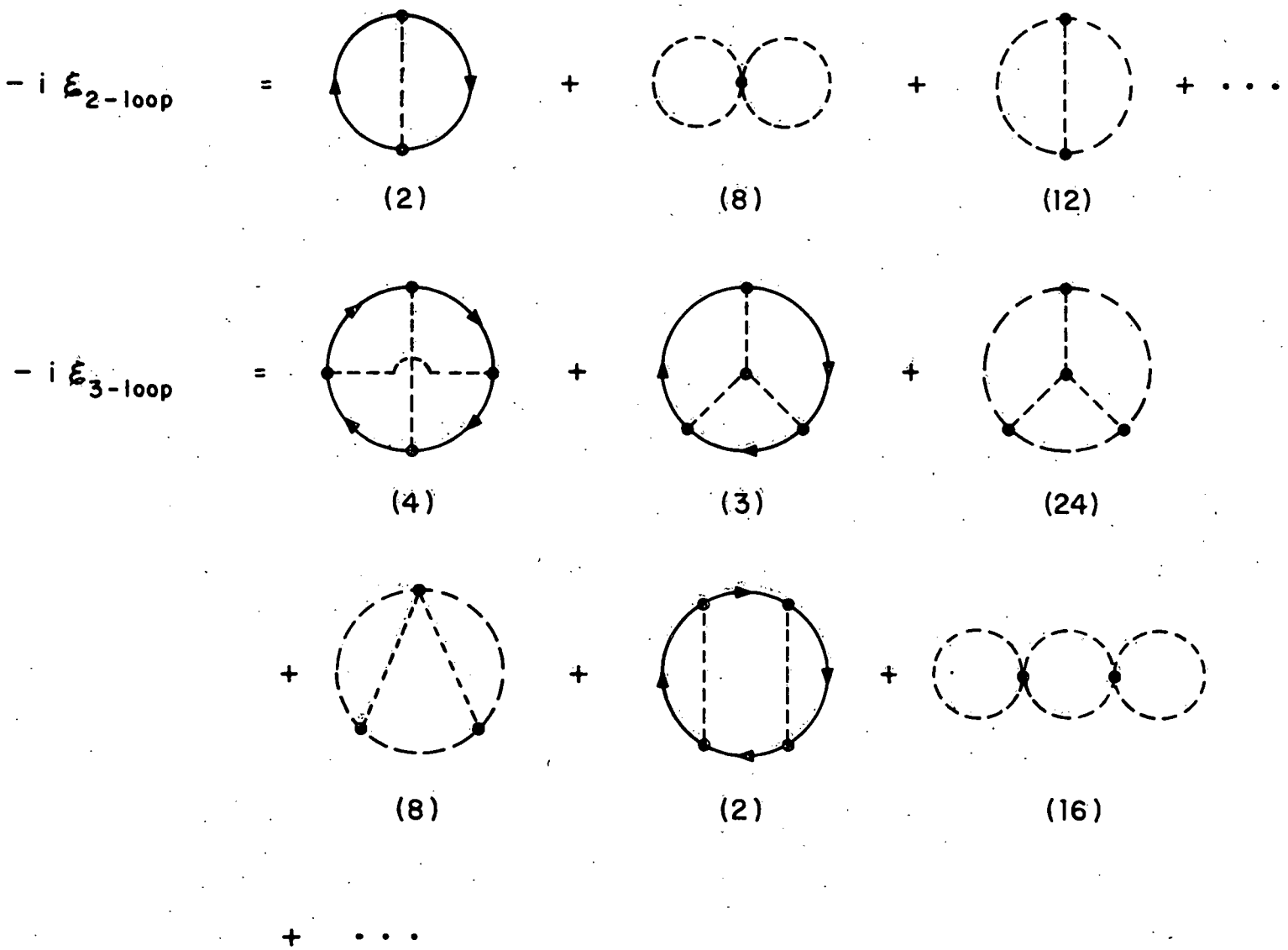

Figure 6

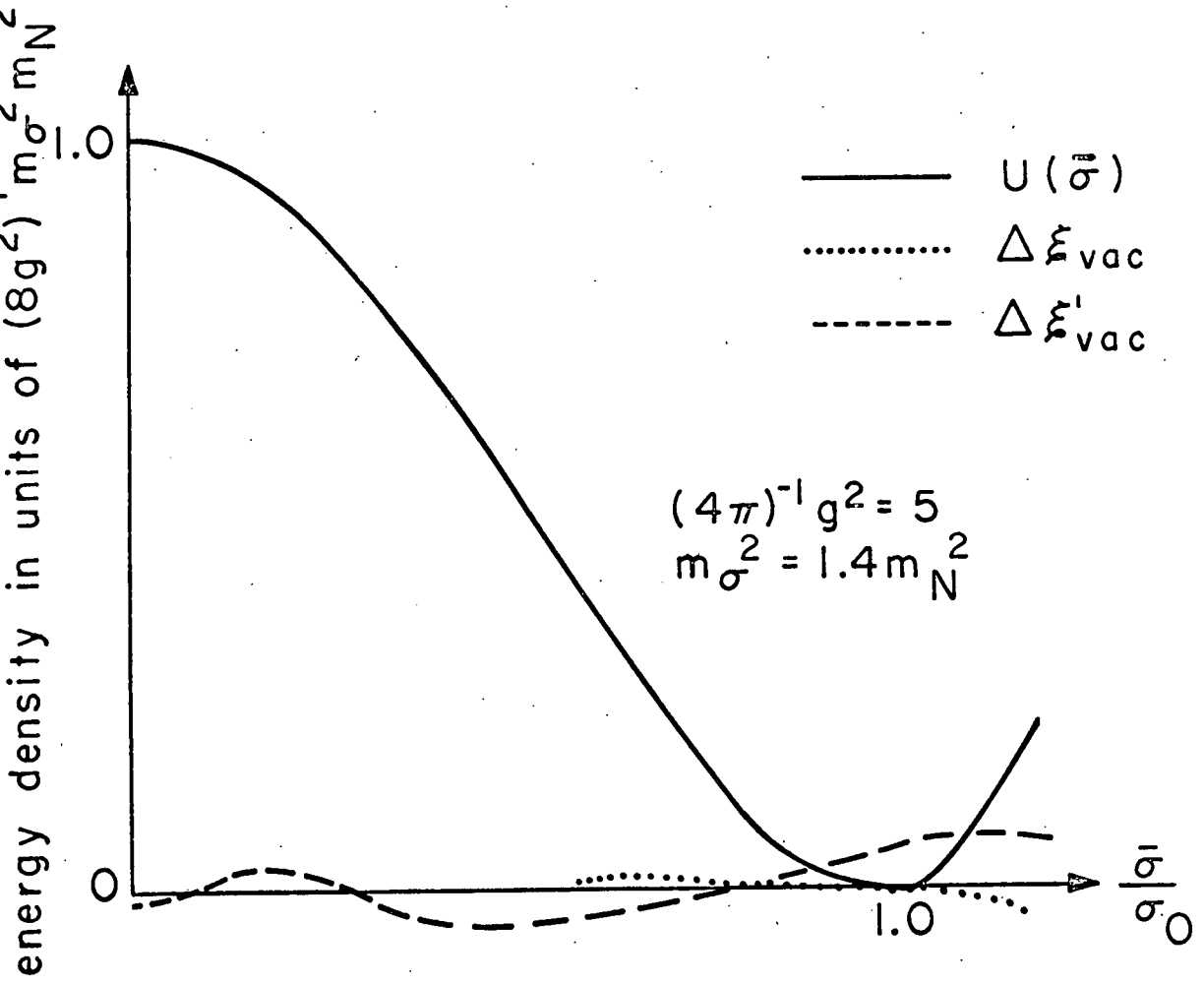
energy density in units of $(8g^2)^{-1} m_\sigma^2 m_N^2$
1.0
0
$U(\vec{\sigma})$
$\Delta\mathcal{E}_{vac}$
$\Delta\mathcal{E}'_{vac}$
$(4\pi)^{-1} g^2 = 5$
$m_\sigma^2 = 1.4 m_N^2$
1.0
$\frac{|\vec{\sigma}|}{\sigma_0}$

Figure 7

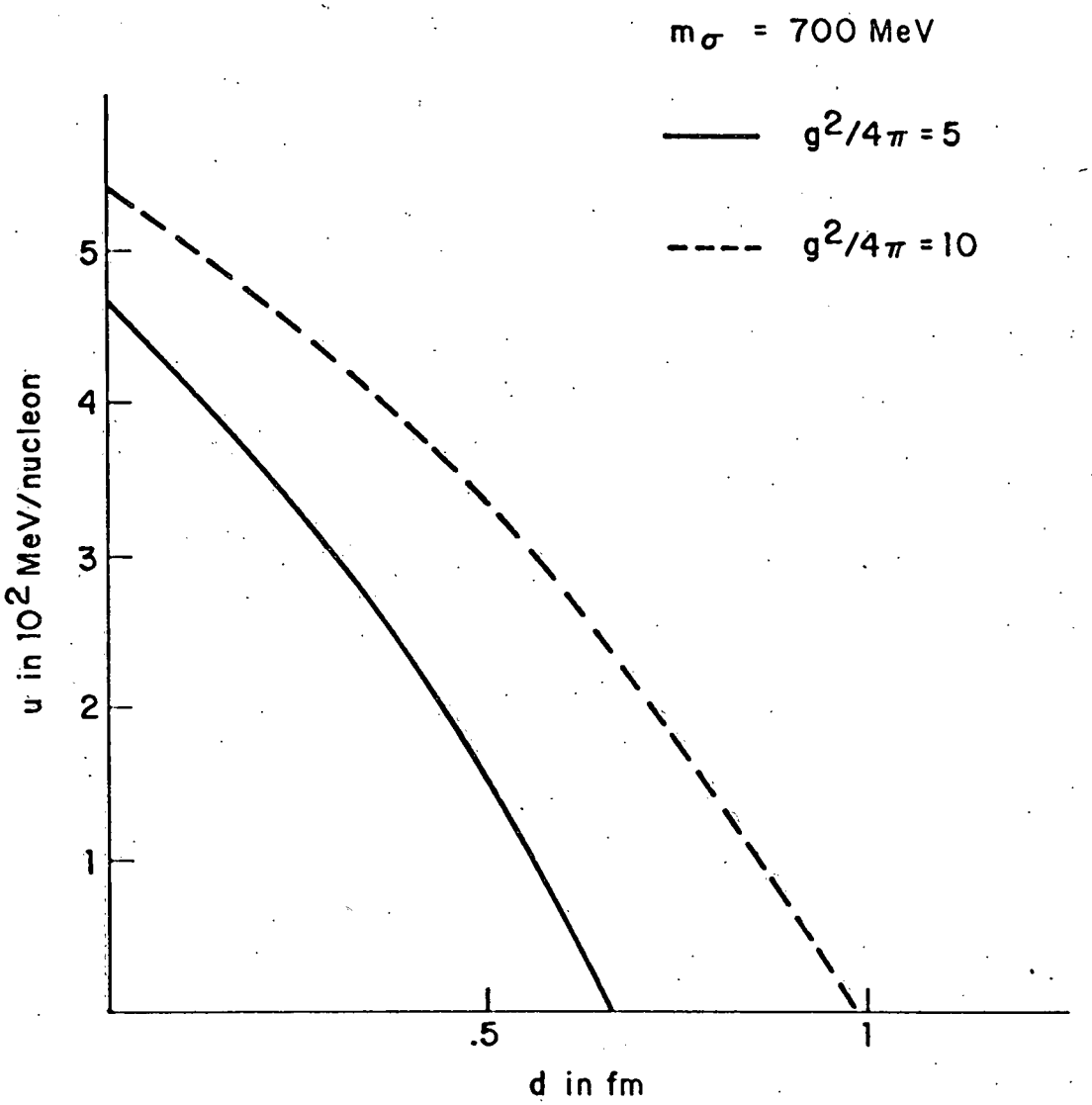
m_σ = 700 MeV
$g^2/4\pi = 5$
$g^2/4\pi = 10$
u in 10^2 MeV/nucleon
5
4
3
2
1
.5
1
d in fm

Figure 8

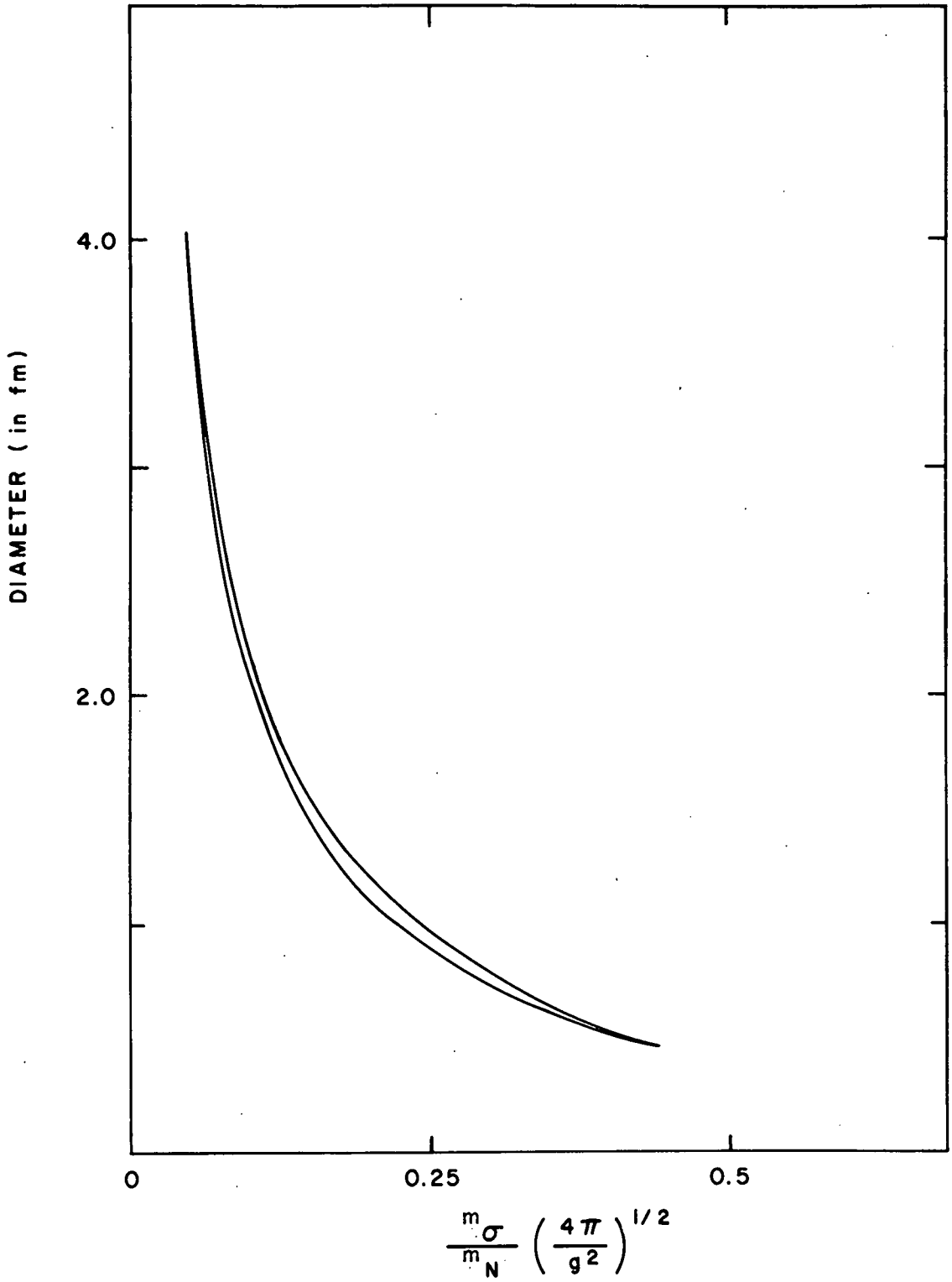
DIAMETER (in fm)
4.0
2.0
0
0.25
0.5
$\frac{m_\sigma}{m_N}\left(\frac{4\pi}{g^2}\right)^{1/2}$

Figure 9